land

Article

Exploring Land Use Management Strategies through Morphological Spatial Patterns Using a Climate–Socioeconomic-Based Land Use Simulation Modeling Framework

Yusong Xie [1,*], Katsue Fukamachi [1,2], Wen Wang [2] and Shozo Shibata [1,2]

[1] Graduate School of Agriculture, Kyoto University, Kyoto 606-8502, Japan; shibata.shozo.6n@kyoto-u.ac.jp (S.S.)
[2] Graduate School of Global Environmental Studies, Kyoto University, Kyoto 606-8502, Japan
* Correspondence: yus_xie@outlook.com; Tel.: +81-9039731116

Abstract: Facing future complex climate changes and global economic fluctuations, land use and land cover (LULC) simulation is recognized as an important initiative to support government decision-making. In this study, a comprehensive LULC simulation modeling framework was proposed based on the PLUS and InVEST models. The Kinki metropolis in Japan was chosen as a case to simulate future LULC changes under four SSP–RCP (126, 245, 370, and 585) scenarios, and to calculate carbon storage (CS) from 2040 to 2100. The results show that cultivated land will decrease while forests will increase, except under scenario SSP585. The artificial surface will increase except under SSP370. The CS changes are significantly correlated with forest area changes. Furthermore, this study highlights the significance of analyzing and discussing future LULCs under wide-area planning. Spatial pattern, morphological spatial pattern analysis (MSPA), and Pearson correlation analysis were used to explore the characteristics of the LULC types. The results reveal that the prefectures within the Kinki metropolitan area can be classified into three groups based on the spatial pattern indices change of the artificial surface. Most cultivated land is concentrated in important patches and corridors (area larger than 40,000 m^2), accounting for over 90% of the total area, while the number is less than 25%. Forests will become more aggregated, and different MSPA classes will have varying impacts on CS changes. This study comprehensively analyzed and validated the feasibility of the simulation results from different LULC perspectives, comparing the similarities and differences in the development of prefectures. Additionally, this research provides a comprehensive framework for integrating simulated LULC types with policy discussions to better guide LULC planning and policy formulation in metropolitan Kinki.

Keywords: land use and land cover simulation; carbon storage; SSP–RCP scenarios; spatial pattern; wide-area planning; the Kinki metropolis

Citation: Xie, Y.; Fukamachi, K.; Wang, W.; Shibata, S. Exploring Land Use Management Strategies through Morphological Spatial Patterns Using a Climate–Socioeconomic-Based Land Use Simulation Modeling Framework. *Land* **2023**, *12*, 1722. https://doi.org/10.3390/land12091722

Academic Editor: Le Yu

Received: 24 July 2023
Revised: 21 August 2023
Accepted: 29 August 2023
Published: 4 September 2023

1. Introduction

The report by the Intergovernmental Panel on Climate Change (IPCC) indicates that human activities, primarily greenhouse gas (GHG) emissions, have led to global climate warming [1]. This warming has significantly altered the structure, function, and processes of ecosystem services, resulting in unpredictable impacts on both global ecology and human beings [2]. Terrestrial ecosystems are now widely acknowledged to play a critical role in global carbon cycle regulation and climate change mitigation, with green spaces being a main factor in terrestrial carbon storage (CS) regulation [3,4]. Changes in land structure resulting from alterations in land use/land cover (LULC) types directly impact vegetation CS and soil carbon levels [5]. The primary cause of LULC changes is urbanization, and worldwide urban expansion creates incentives to convert green spaces into artificial surfaces [6,7]. Consequently, studies on LULC changes contribute to a better knowledge of urban development processes, ecosystem services, and provides a foundation for land development and management [8–10].

Future LULC simulations are considered an important initiative that provide a scientific basis for supporting governmental decision-making. Moreover, they have the potential to promote environmentally sustainable development and protection [11]. In scenario selection, scenarios that describe the possible future development of anthropogenic drivers of climate change, aligned with socioeconomic development, are critical [12]. The Coupled Model Inter-comparison Project Phase 6 (CMIP6), launched in 2013 by the World Climate Research Program (WCRP) and its core project, the Working Group on Coupled Modeling (WGCM), served as an essential scientific resource for the IPCC to assess and synthesize the latest climate science and inform global climate policy discussions [13]. The CMIP6 links shared socioeconomic pathways (SSP) to representative concentration pathways (RCP) used in the CMIP5, generating a range of future climate scenarios, namely the SSP–RCP [14,15]. Notably, researchers have widely applied SSP–RCP scenarios in LULC simulation studies to explore the characteristics of LULC change [16–19]. In addition, several methodologies have been commonly used in LUCC simulations, including the Land Change Modeler, the Conversion of Land Use and its Effects model, the Meta-cellular Automata, the Future Land Use Simulation model, and the Patch Generation Land Use Simulation (PLUS) model [5,11,20–22]. In this study, the PLUS model was used, which was combined with the cellular automata (CA) model based on multiclass random patch seeding, to better simulate changes in the level of multiclass LULC patches [22]. It improves the accuracy of simulating changes in LULC distribution. In addition, this model can compare and identify the influence of various driving factors on LULC changes [23].

Over the past five years, there has been a significant increase in study focusing on predicting future LULC changes [24]. However, the majority of studies focus on cities in developing countries; fewer studies have explored the patterns of LULC change and simulation prediction in cities in developed countries [2,22]. Urban development in developed countries provides valuable insights into the dynamics of LULC patterns, the effectiveness of LULC policies, and the complex interplay among urbanization, socioeconomic factors, and environmental considerations. The experiences learned from developed countries can provide valuable guidance for adjusting LULC policies and informing future LULC planning in both developed and developing countries. Furthermore, there is often a lack of institutional fit-related analyses. Most studies have focused on future ecosystem services evaluation and landscape patterns change, overlooking the specific planning requirements and legal framework of the studied areas [4,25]. Particularly for some developed countries like Japan and the United Kingdom, artificial surface development and management are subject to strict legal regulations and planning constraints [26].

The Basic Act for Land, the National Spatial Planning Act, and the National Land Use Planning Act create a comprehensive set of territorial planning legislation in Japan (Figure S1). This study focuses on conducting extensive LULC simulations and discussions in the Kinki metropolis of Japan. As the limitations stemming from the long-term concentration of development in the Tokyo metropolitan area become more evident, being the second-largest economy in Japan, the Kinki metropolis is presented with amplified opportunities for urban growth and the reinvigoration of social capital (Kansai Greater Regional Plans). Nevertheless, in comparison to other metropolitan regions across Japan [27], research addressing LULC changes and their management remains inadequate in the Kinki metropolis. Within the context of territorial planning legislation, the Kinki metropolitan development plans, as well as national park and green space preservation plans, provide essential guidance for future wide-area LULC development and management. Additionally, in response to the challenges of an aging population and other emerging issues [28,29], the agricultural land conversion permit system is implemented to restrict the conversion of agriculturally productive land with high output or large areas into other LULC types, in order to address the decline in cultivated land availability. Land management through morphological characteristics is still the most common method, although the spatial division considered various factors, such as the regional economy and population structure. In addition, the formulation and implementation of laws have certain foresight, so the analysis of land use simulation and simulation results has reference value for the formulation and implementation of regional policies to a certain extent.

Morphological spatial pattern analysis (MSPA) has been extensively incorporated into the principles of geographically based landscape ecology [30], and it is more commonly conducted in the field of ecological function assessments, network construction, and the connectivity of green infrastructure [31,32]. MSPA is an image processing method based on mathematical morphology [33], which can divide LULC types according to morphological characteristics. Furthermore, the utilization of MSPA complements the quantitative analysis of spatial patterns based on the landscape pattern index [34]. It can provide information on the spatial patterns, ecological functions, and areas in LULC changes.

Based on the background, this study focuses on the Kinki metropolitan area, and aims to conduct LULC simulations under four future SSP–RCP scenarios from the CMIP6. These scenarios considered variations in the population, economy, climate characteristics, and LULC demands. Furthermore, this study places particular emphasis on exploring and discussing the spatial patterns under the basis of wide-area planning. The primary objectives of this study are as follows: (1) to simulate LULC from 2020 to 2100; (2) to analyze changes in the distribution of terrestrial CS under four scenarios and explore their correlation with the MSPA classes of forest; and (3) to analyze and discuss the spatial pattern changes of LULC types guided by wide-area planning. This study will contribute to a comprehensive understanding of the future dynamic changes in the LULC in the Kinki metropolis, emphasizing the significance of formulating localized land management strategies and providing valuable references for policymakers, landowners, and land managers.

2. Study Area and Materials

2.1. Study Area

Metropolitan Kinki, which comprises six prefectures (regional authorities comprising municipalities) including Osaka, Kyoto, Hyogo, Nara, Shiga, and Wakayama, is the second-largest economic region in Japan (National Spatial Strategy) (Figure 1). This metropolis plays a crucial role in Japanese politics, economy, culture, and global communication (Kansai Greater Regional Plans). Its total area is approximately 27,329.71 km^2, with a population of 20,554,346 people as of 2020, accounting for 16.28% of the total population of Japan [35]. The Kinki metropolis is located in central and western Honshu, Japan, and is surrounded by mountains, the Sea of Japan to the north, the Seto Inland Sea to the west, and the Pacific Ocean to the south (Figure 1). Its geography is diverse, with rugged terrain around the central lowland such as Osaka Plain, Kyoto Basin, Nara Basin, and Omi Basin, and the largest lake of Japan, Lake Biwa, located in the northeastern area. There are regional differences due to the amount of precipitation and its seasonal distribution due to the relationship with the topography and the ocean, which includes Japan's representative climate types. The main climate zones are divided into the Sea of Japan climate in the northern part and the Pacific coastal climate in the southern part. The Pacific coast-type climate is further subdivided into the Nankai climate zone, the Tokai climate zone, and the Setouchi climate zone.

In the 21st century, metropolitan Kinki, like other Japanese regions, is also facing various challenges like a declining population, significant aging, economic stagnation, and a reduction in regional status and urban vibrancy, which are of widespread concern. As a consequence of these factors, the LULC change in this region has been slower from 2000 to 2020, with the LULC types with the larger areas and more significant changes being cultivated land, forests, and artificial surfaces (Figures 1 and 2). Nevertheless, the Kansai Greater Regional Plans has proposed to establish the Kinki metropolitan area as the core of Japan's future economic growth and enhance its vitality. This plan presents both opportunities and challenges for regional development, making the future LULC trajectory worthy of attention under the complex economic development and climate change.

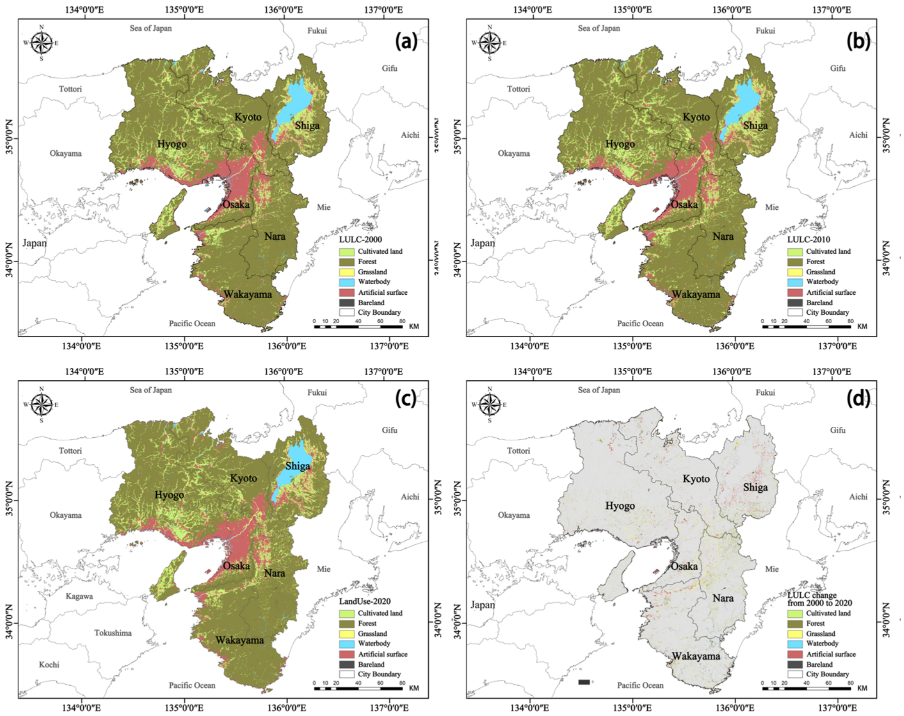

Figure 1. The LULC map of metropolitan Kinki and the LULC changes from 2000 to 2020 ((**a**) LULC in 2000, (**b**) LULC in 2010, (**c**) LULC in 2020, (**d**) LULC change from 2000 to 2020).

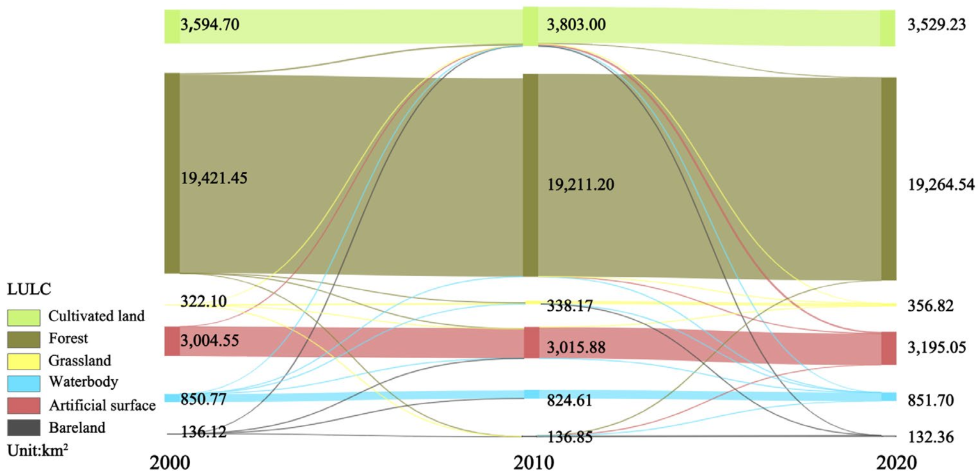

Figure 2. LULC changes in metropolitan Kinki from 2000 to 2020.

2.2. Data Acquisition

The boundary shapefile of the Kinki metropolis was obtained from the Ministry of Land, Infrastructure, Transport, and Tourism (https://nlftp.mlit.go.jp/ksj/, accessed on 10 September 2022), and the land dataset was obtained from GLOBELAND30 (http://www.globallandcover.com/, accessed on 25 September 2022). Based on previous studies and the consideration of a comprehensive selection of driving factors, we selected a total of 25 driving factors (Table 1), including 3 topographic factors, 2 climatic factors, 9 soil factors, 2 socioeconomic factors, and 9 spatial accessibility factors. After a series of data preprocessing steps in ArcGIS 10.5 software, including projection transformation, Euclidean distance, resampling, and clipping—all of the above data were converted to raster data with the same projected coordinate system and a spatial resolution of 30 m (Figure S2).

In this study, data on population density, GDP density, temperature, and precipitation were collected for four scenarios in 2040, 2060, 2080, and 2100, which were used as driving factors for LULC simulation. The population density and GDP density data were obtained from kilometer-scale grid data of future climate change scenarios from SSPs [3,36]. Future temperature and precipitation data were obtained from WorldClim 2.1 based on the MRI-ESM2-0 model (http://worldclim.org/, accessed on 22 January 2023).

Table 1. Data sources and processing.

Category	Data	Year(s)	Original Resolution	Data Resource
Land dataset	Land use/cover data	2000, 2010, 2020	30 m	GLOBELAND30 (http://www.globallandcover.com/, accessed on 25 September 2022)
Topographic factors	DEM	2022	30 m	JAXA-DEM (https://www.eorc.jaxa.jp/ALOS/en/aw3d30/, accessed on 13 October 2022)
	Slope		30 m	
	Aspect		30 m	
Climate factors	Annual mean precipitation	2000–2018	30 arc-sec	WorldClim 2.1 (https://www.worldclim.org/, accessed on 16 November 2022)
	Annual mean temperature		30 arc-sec	
Soil characteristics	soil type	2011	30 m	National Agriculture and Food Research Organization (https://soil-inventory.rad.naro.go.jp/offer.html, accessed on 28 November 2022)
	Soil water capacity	2017	250 m	ISRIC-World Soil Information (https://data.isric.org/, accessed on 10 December 2022)
	Depth to bedrock		250 m	
	Cumulative probability of organic soil		250 m	
	Soil organic carbon stock		250 m	
	Soil PH		250 m	
	Texture class		250 m	
	Sand content		250 m	
	Clay content		250 m	
Socioeconomic factors	GDP density	2015	5 km	[37]
	Population density	2020	100 m	
Spatial accessibility	Proximity to town hall	2022	30 m	WorldPop (https://hub.worldpop.org/, accessed on 21 December 2022) OpenStreetMap (https://download.geofabrik.de/, accessed on 21 December 2022)
	Proximity to residential		30 m	
	Proximity to transportation node		30 m	
	Proximity to railway		30 m	
	Proximity to trunk/motorway		30 m	
	Proximity to primary road		30 m	
	Proximity to secondary road		30 m	
	Proximity to tertiary road		30 m	
	Proximity to open water		30 m	

The driving factors collected were allowed to be inconsistent with the time period of the land use data, but the time period was as close as possible to the time period of the LULC data [4].

3. Methodology

This study has three parts: (1) Future LULC simulations under four SSP–RCP scenarios, (2) carbon storage calculation by future LULC, (3) Spatial patterns analysis and morphological spatial patterns from the perspective of LULC types (Figure 3).

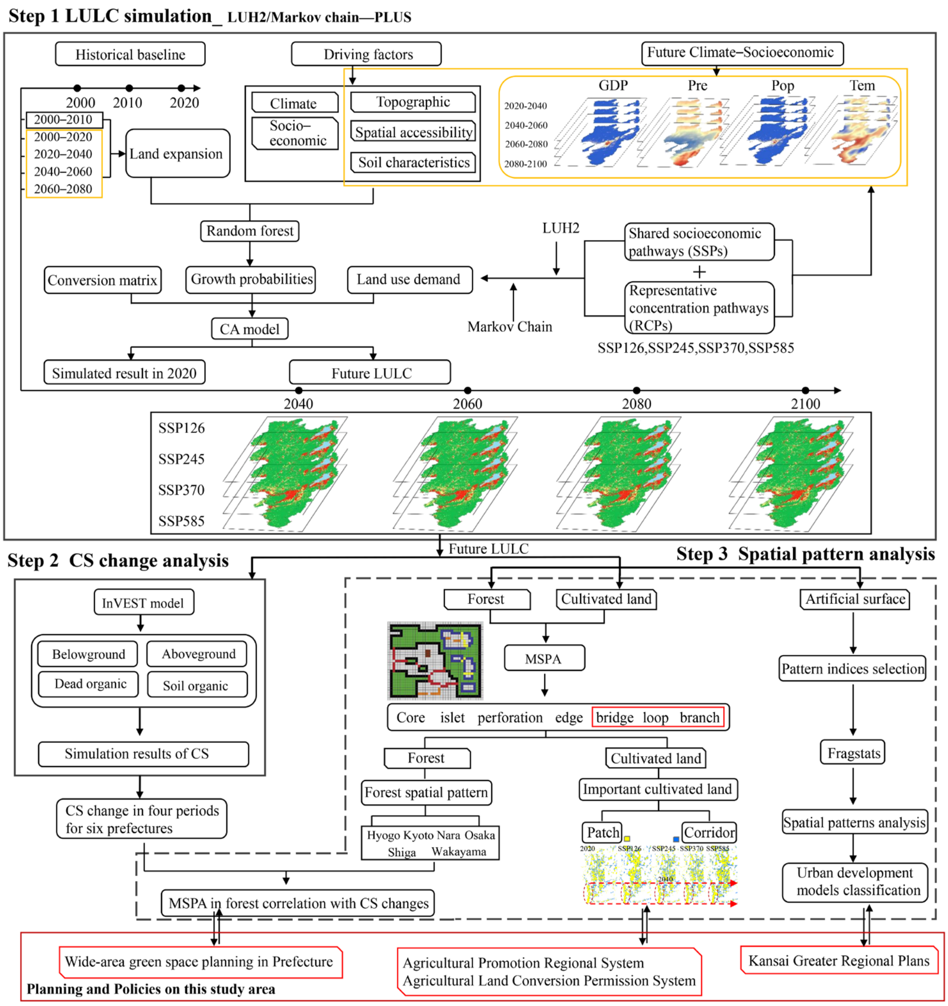

Figure 3. Technical analysis pathway and modeling framework.

3.1. Future LULC Scenarios

3.1.1. LULC Demand from LUH2-Markov Chain

This study selected the basic scenarios for climate model projections in Tier 1 (SSP126, SSP245, SSP370, and SSP585) of the Scenario Model Inter-comparison Project [15,38]. SSP126, which combines SSP1 and RCP2.6, represents a scenario characterized by low GHG emissions resulting from a sustainable development trajectory. SSP245, combining SSP2 and RCP4.5, emphasizes development that aligns closely with historical patterns without significant deviations. SSP370, comprising SSP3 and RCP7.0, reflects a regional rivalry and barriers to international trade scenario with high GHG emissions, and the economic development is slow, with inequalities that persist or worsen over time. SSP585, involving SSP5 and RCP8.5, depicts a future where global development is rapid, primarily fueled by fossil fuel-based, energy-intensive economies, leading to substantial GHG emissions (Table S1) [14,39].

Land-Use Harmonization2 (LUH2; http://luh.umd.edu/, accessed on 30 October 2022) is an important part of the CMIP6; it presents eight LULC scenarios at 0.25° × 0.25° resolution. To obtain the high-resolution simulation results, this study quantified and calibrated each LULC scenario in LUH2 with the historical LULC in 2020, while retaining the original fluctuation rates of LULC types in LUH2 [19,38]. Furthermore, using the historical LULC data in 2020, the SSP–RCP scenarios of land use demand trajectories were obtained. In addition, considering the substantial inaccuracy in grassland due to the low resolution in LUH2 and the missing results of the water body [19,38], this study used a Markov chain to rectify the LULC demand data, and determined the land use demand trajectories in the Kinki metropolis (Figure 4).

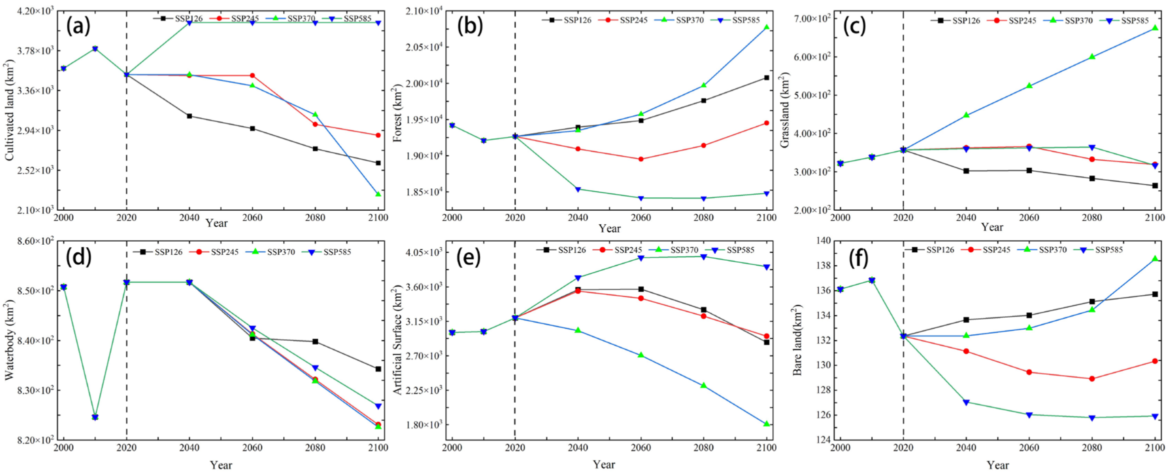

Figure 4. Trajectories of land use demand, which were calibrated based on the 2020 land use map ((**a**) cultivated land, (**b**) forest, (**c**) grassland, (**d**) waterbody, (**e**) artificial surface, (**f**) bare land).

3.1.2. Spatiotemporal Dynamic Simulation Based on PLUS

The PLUS model contains two modules: (1) a rule-mining framework based on a land expansion analysis strategy (LEAS); and (2) a CA based on multi-type random patch seeds (CARS) [23]. Firstly, the LULC maps of two periods were overlaid to extract the cells representing the change areas. Then, the LULC expansion map was used as a transition analysis strategy in the LEAS. The random forest classifier (RFC) algorithm was applied to identify the relationship between the changing area and every driving factor. This process helped determine the contribution value of the driving factors to the change in each LULC type during the two periods [36]. Finally, a growth mechanism based on CARS was utilized to dynamically simulate various types of land patches.

3.1.3. Model Evaluation

This study used the LULC in 2000 and 2010 to simulate LULC in 2020, and then compare the simulated 2020 results with the actual 2020 results to verify the accuracy of the simulation results. Two evaluation metrics, the overall accuracy and Kappa coefficient, were employed. The overall accuracy measures the ratio of correctly classified cells to the total number of classes. On the other hand, the Kappa coefficient ranges from 0 to 1. Generally, a Kappa coefficient greater than 0.6 indicates acceptable results, while a value above 0.8 suggests a relatively accurate simulation outcome [40].

$$\text{Kappa} = \frac{p_0 - p_c}{p_p - p_c} \tag{1}$$

where p_0 and p_c refer to the actual and predicted simulation accuracy in a random state, respectively, and p_p is the proportion of correct simulations in the ideal classification case and is commonly assumed to be 1.

In this study, the calculated Kappa coefficient was found to be 0.92, indicating a high level of agreement between the simulated and actual LULC data. Additionally, the overall accuracy was determined to be 0.96, further confirming the reliability and accuracy of the simulation method employed in this study (Table S2). These results demonstrate that the method used in this study meets the operational requirements of the model, and can effectively simulate LULC changes.

3.2. CS Estimation Based on the InVEST Model

The Integrated Valuation of Ecosystem Services and Tradeoffs (InVEST) model is commonly employed to simulate and analyze the connections between nature and human well-being, including ecosystem services or the contributions of nature to people [41,42].

One of the most commonly used models in InVEST is the carbon storage and sequestration model, which aggregates the amount of carbon stored in four pools based on LULC maps and the statistics of previous studies (Table 2) [41,42].

$$C = \sum_{t=1}^{n} S_t \times (C_{t,a} + C_{t,b} + C_{t,c} + C_{t,d}) \quad (2)$$

where C is the total CS; S_t refers to the area of cropland, forest, grassland, waterbody, artificial surface, and bare land (km^2); $C_{t,a}$, $C_{t,b}$,$C_{t,b}$, and $C_{t,d}$ are the carbon densities from aboveground, belowground, soil organic, and dead organic matter, respectively, of the t type of LULC (Mg/km^2).

Table 2. Carbon densities of each land use/land cover type (Mg/km^2).

Land Use Types	Aboveground Carbon Density	Belowground Carbon Density	Soil organic Carbon Density	Dead Organic Matter Density	Sources
Cultivated land	21.00	2.52	73.20	2.52	[43–45]
Forest	84.60	20.30	90.00	7.01	[43,46–48]
Grassland	2.91	4.65	114.00	0.00	[43,49]
Bare land	0.20	0.00	40.10	0.00	[3,50]

3.3. Spatial Pattern Analysis from the Perspective of LULC Types

3.3.1. Spatial Pattern Analysis of Artificial Surface

Landscape pattern indices are crucial indicators for analyzing the fragmentation, shape characteristics, aggregation, and shape diversity of LULC patches [51]. These indices are commonly employed to quantitatively analyze ecological landscape patterns [52,53]. By considering the calculation principles through the spatial distribution of patches, we utilized several landscape pattern indices, namely the Largest Patch Index (LPI), Landscape Shape Index (LSI), Contagion (CONTAG), and Shannon's diversity index (SHDI) to analyze the fragmentation, shape, degree of aggregation, and shape diversity of future artificial surface patches. We aimed to explore the spatial pattern under different scenarios. The calculations of all the indices were conducted using Fragstats 4.2 software.

3.3.2. Changes in Morphological Patterns of Green Space

MSPA was employed to divide the LULC map into seven MSPA classes, based on the Euclidean distance threshold between raster cells [54,55] (Table 3). It can provide insights into the extraction of LULC patches using mathematical morphology [56]. This study took one type of LULC as the foreground and the remaining categories as the background; then, these data were converted into raster data in TIFF format. Eight-neighbor connectivity and edge width values of 20 were used in this research, in order to obtain more detailed information at the regional scale in different land use types as much as possible [34]. Additionally, considering the pixel size and the need for significant MSPA classes for each LULC type in each period, the edge width was uniformly set at 4 m [34,56]. The following equation was used to calculate the cover area of each MSPA class.

$$S_{ti} = S_t \times P_i (i = 1, 2, \ldots, 7) \quad (3)$$

where S_t refers to the area of cultivated land and forest (km^2); P_i represents the proportion of different MSPA classes under a specific LULC type (%); S_{ti} refers to the area of core, islet,. . ., branch under a specific LULC type (km^2).

Table 3. Definitions of MSPA classes.

MSPA Classes	Definition
Core	Large area patches that exceed the specified edge width distance from the background
Islet	Patches that are smaller than the core and exist in the background as isolated and fragmented forms
Edge	External perimeter of core area
Perforation	The internal perimeter of the core area refers to the boundary within the core where one land use type is encroached upon by other land use types, creating a similar hollow feature
Bridge	The corridor connecting different cores
Loop	Internal corridor connecting the same core
Branch	Only one end is connected to the foreground, striped land with low connectivity

3.3.3. Identification of Important Cultivated Land Patches and Corridors

In response to the decline in cultivated land, Japan has implemented a series of initiatives to protect and regulate its use. Notably, the Agricultural Promotion Regional System and the Agricultural Land Conversion Permission System specifically address the management of cultivated land exceeding 40,000 m^2. Development activities on such land require local approval following consultation with the Minister of Agriculture, Forestry, and Fisheries. Although evaluating the functionality of cultivated land requires a comprehensive analysis of various factors such as soil composition, crop yield, and market demand, area-based management is considered one of the most direct and effective approaches. This study focused on identifying important cultivated land larger than 40,000 m^2, and explored its morphology through patches and corridors classification. Within the MSPA framework, the core, islet, edge, and perforation correspond to patches, while the bridge, loop, and branch represent corridors [57]. ArcGIS was used to further count and extract the areas and numbers of cultivated land patches and corridors above 40,000 m^2.

3.3.4. The Correlation between MSPA Classes in Forest and CS Changes

This study utilized Pearson correlation analysis to explore the relationships between CS changes and MSPA class changes of forest. In conducting this analysis, a crucial step is to select variables for statistical analysis to determine the significance of the correlation coefficient © and identify tradeoffs. In this study, it was determined that there is a strong linear correlation when the absolute value of r exceeds 0.4, This threshold serves as a guideline for evaluating the strength and direction of the correlation between CS changes and MSPA class changes, providing insights into the relationship between forest characteristics and carbon storage dynamics.

4. Results

4.1. Future LULC under Different Scenarios

The future LULC results indicate that except for SSP370, which exhibited significant grassland changes, the primary types of LULC change were cultivated land, forests, and artificial surfaces (Table 4). In terms of cultivated land, it showed a trend of growth followed by stabilization in the SSP585, but the other three scenarios exhibited a decline from 2020 to 2100. SSP370 experienced the most substantial decline, with only two-thirds of the cultivated land area in 2020. In contrast, the SSP585 remained stable after initially increasing to 541.99 km^2 in 2040. Overall, the forest areas in SSP126, SSP245, and SSP370 increased from 2020 to 2100, with the growth areas exceeding 800 km^2, except for a decline in SSP585. Artificial surface areas increased in all of the scenarios by 2100, except for SSP370, which experienced a decrease of roughly 660 km^2. Under SSP126, the artificial surface area reached 3569.00 km^2 in 2060, and then began to decrease to 3427.89 km^2 in 2100. Both

SSP245 and SSP585 showed an increase in artificial surface area from 2020 to 2100, with SSP585 growing by about 670 km^2.

Table 4. Statistics in LULC under four scenarios.

Time	Scenario	Cultivated Land/km^2	Forest/km^2	Grassland/km^2	Waterbody/km^2	Artificial Surface/km^2	Bare Land/km^2
2040	SSP126	3091.84	19,369.78	325.54	850.61	3558.43	133.49
	SSP245	3512.60	19,069.68	361.53	850.61	3404.31	130.96
	SSP370	3522.68	19,322.06	445.96	850.61	3056.18	132.20
	SSP585	4071.22	18,515.44	359.67	850.61	3405.86	126.89
2060	SSP126	2993.92	19,484.09	303.38	845.28	3569.00	134.01
	SSP245	3514.56	19,048.89	346.53	841.33	3448.95	129.45
	SSP370	3410.46	19,572.82	523.55	841.17	2862.40	119.29
	SSP585	4076.42	18,417.96	362.18	842.51	3504.59	126.04
2080	SSP126	2746.04	19,760.55	282.73	839.77	3567.81	132.80
	SSP245	3249.17	19,141.93	332.31	832.17	3645.21	128.91
	SSP370	3103.17	19,968.86	599.40	831.83	2723.55	102.89
	SSP585	4076.42	18,412.77	338.44	834.61	3541.65	125.81
2100	SSP126	2595.63	20,078.15	263.49	834.28	3427.89	130.25
	SSP245	2888.57	19,452.38	318.67	823.11	3716.64	130.33
	SSP370	2439.17	20,769.84	674.59	822.59	2535.69	87.82
	SSP585	4076.42	18,119.78	316.38	826.89	3864.29	125.93

The LULC expansion maps show that despite varying types of LULC changes, there were similarities in the change areas and severity (Figure 5). For instance, along Lake Biwa in Shiga Prefecture, the southeast area's LULC changes were apparent in all four scenarios. Except for SSP370, which increased forest area, the rest showed mainly artificial surface expansion. In the north of Wakayama, artificial surface expansion occurred under all four scenarios. This study further extracted and calculated LULC changes from 2020 to 2100 under six prefectures by administrative division (Figure 6). The results revealed varied LULC changes among the prefectures. For example, cultivated land decreased in all prefectures except Osaka under the SSP126 scenario, with the largest decrease observed in Shiga. The artificial surface area increased only in Hyogo and Shiga, with a significant increase in Shiga. The main types of LULC changes differed by prefecture. Under SSP370, Hyogo, Kyoto, and Shiga are characterized predominantly by cultivated land and artificial surface conversion to forest. Nara's only grassland area increased under this scenario, with all other LULC types converting to grassland.

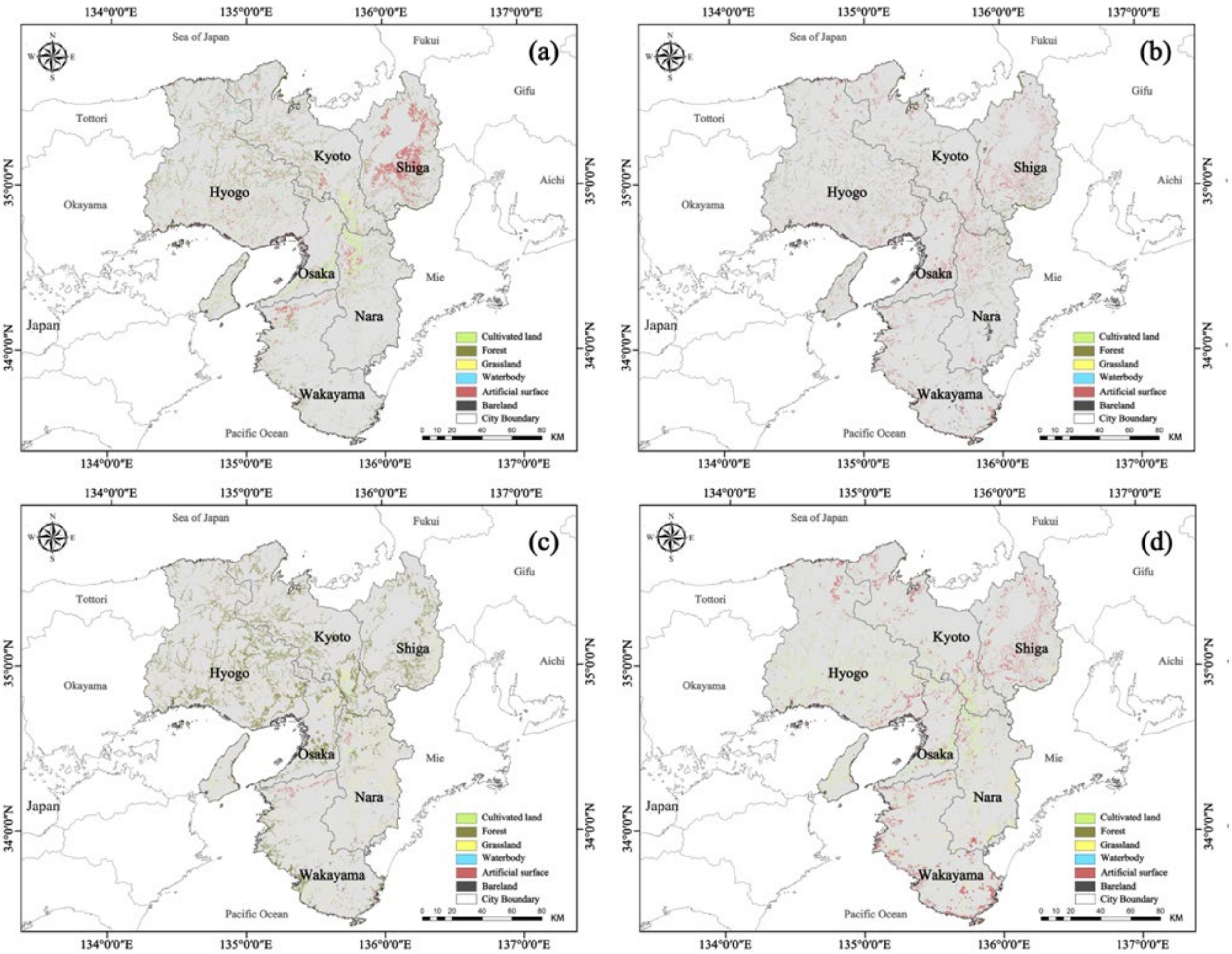

Figure 5. Land use expansion map from 2020 to 2100 under four scenarios ((**a**) SSP126; (**b**) SSP245; (**c**) SSP370; (**d**) SSP585).

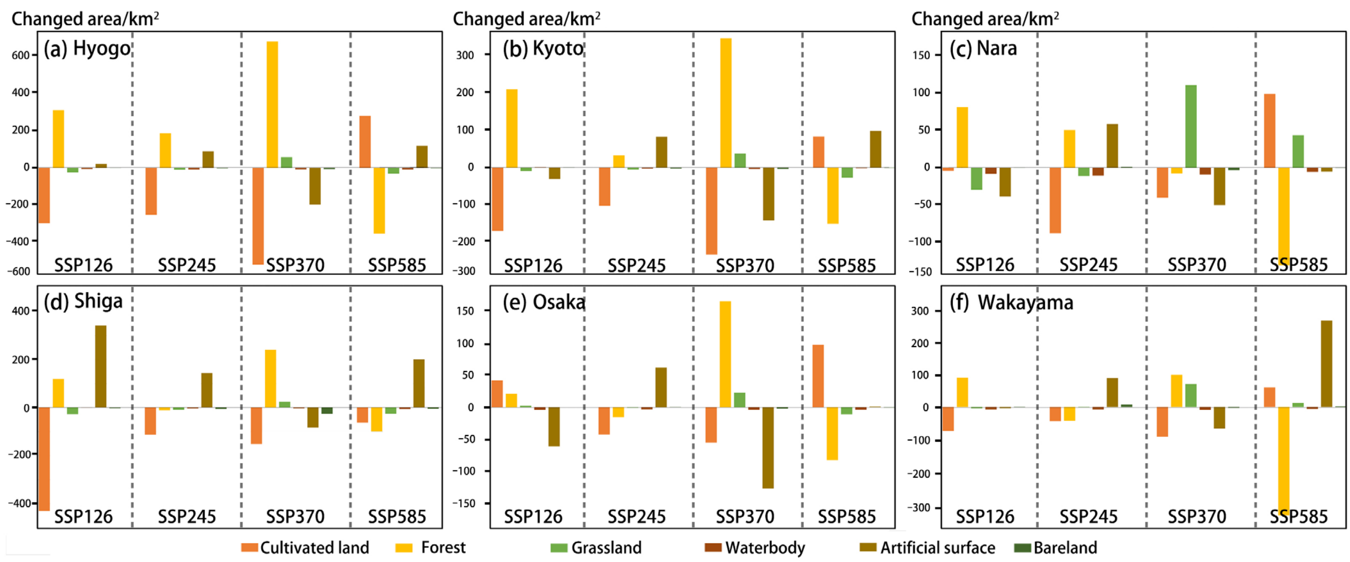

Figure 6. LULC changes from 2020 to 2100 in six prefectures.

4.2. CS for LULC under CMIP6 Scenarios

The CS results indicate a significant variation in CS levels under different scenarios (Table 5, Figure 7). CS continues to decrease under SSP585, primarily due to forest decline and the expansion of artificial surfaces. Conversely, the total CS increases in SSP126 and SSP370, mainly due to forest increase, with SSP370 having the highest annual growth rate of 0.29 Tg (10^6 Mg) associated with the rapid shrinkage of artificial surfaces. The SSP245 scenario results show a steady decrease in CS from 2040 to 2080, followed by a recovery period after 2080, with fluctuations in CS compatible with forest changes. Furthermore, this study calculated the CS in each prefecture under the four scenarios (Figure 8). In the SSP126 scenario, although CS increased in all of the prefectures, the magnitude of the increase varied considerably. Hyogo exhibited the highest increase of 3.12 Tg, while Osaka had a modest increase of only 0.37 Tg. Under the SSP245 scenario, the overall CS in Osaka and Shiga decreased, while Kyoto, Nara, and Wakayama experienced slight increases in total CS by 2100, although the changes between 2040 and 2100 were inconsistent. Notably, Hyogo demonstrated the highest growth of 1.88 Tg. In the SSP370 scenario, all of the cities observed an increase in CS, with Hyogo experiencing the most significant rise of 8.64 Tg, and Nara showing a modest increase of 0.70 Tg. In contrast, under the SSP585 scenario, all cities exhibited low CS levels, which decreased between 2040 and 2100. Wakayama experienced the most notable decrease of 2.83 Tg.

Table 5. CS dynamic change from 2020 to 2100.

Scenario	Total CS (Tg)				CS Change (Tg)				
	2040	2060	2080	2100	2020–2040	2040–2060	2060–2080	2080–2100	2020–2100
SSP126	426.30	427.37	430.24	434.92	−2.36	1.07	2.87	4.68	6.26
SSP245	424.85	424.26	423.33	425.86	−3.81	−0.59	−0.93	2.53	−2.80
SSP370	431.08	435.92	441.72	452.16	2.41	4.84	5.80	10.44	23.50
SSP585	419.16	417.27	416.88	410.69	−9.50	−1.89	−0.39	−6.18	−17.97

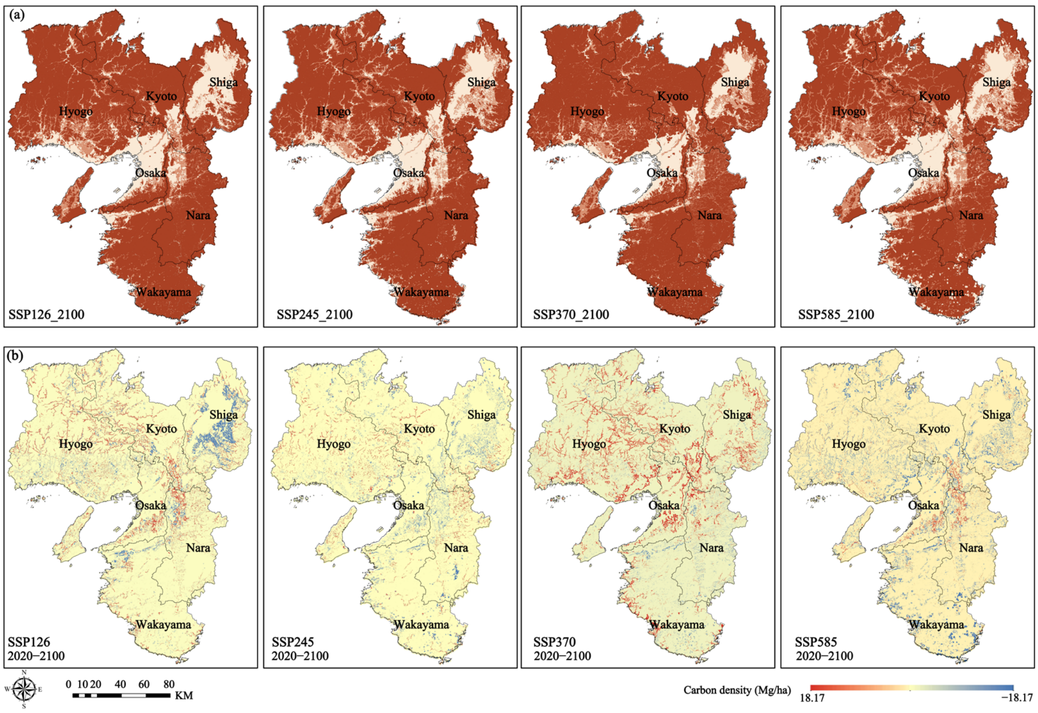

Figure 7. CS in 2100 (**a**) and the distribution changes from 2020 to 2100 (**b**) under four scenarios.

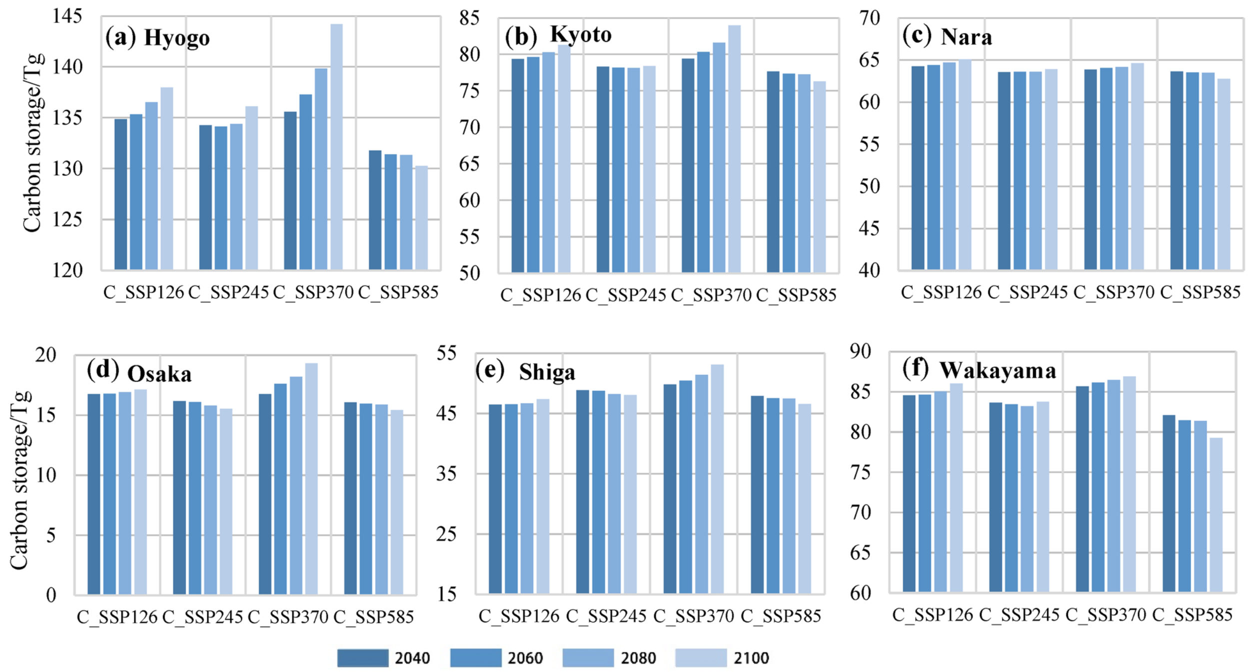

Figure 8. CS dynamic change of prefectures in metropolitan Kinki.

4.3. The Spatial Patterns of Artificial Surface Changes

In the different simulated periods, the four scenarios exhibited disparities in their changes in spatial pattern indices for artificial surface patches (Figure 9). For instance, under the SSP126 scenario, the LPI and CONTAG indices in Wakayama decreased during the 2000–2040 period, remained stable in 2040–2080, and increased in 2080–2100. These results indicate that the artificial surface area in Wakayama becomes increasingly fragmented during 2000–2040, but shows aggregated development by 2080–2100.

Furthermore, the artificial surface patch distributions in the six prefectures are different by 2100. In Hyogo, Shiga, and Wakayama, the change in spatial pattern indices remained largely consistent, with the trend from 2000 to 2020 under the SSP126, SSP245, and SSP585 scenarios. The LPI and CONTAG show a decreasing trend in all of the scenarios except for SSP370, while the value of the LSI and SHDI increased. These findings indicate that the fragmentation of artificial surface patches increases in the SSP126, SSP245, and SSP585 scenarios, and the shapes of the patches become more complex and less aggregated.

In Kyoto and Nara, there are similarities in terms of changes in the spatial pattern indices. The LPI and CONTAG decreased in the SSP245 and SSP585 scenarios, while the SHDI increased. The results show increased fragmentation of artificial surface patches and decreased aggregation by 2100, while the situation is the opposite for SSP126 and SSP370.

In the SSP126, SSP370, and SSP585 scenarios, the LPI, CONTAG, and SHDI indices fall in Osaka, while the LSI index rises. This indicates that by 2100, artificial surface patches will be fragmented, more complex and diversified in shape, and less aggregated. Under the SSP245 scenarios, the LPI and LSI rise while the other indices fall. These scenarios show large patches of artificial surface expansion, and also an increase in fragmented artificial surfaces.

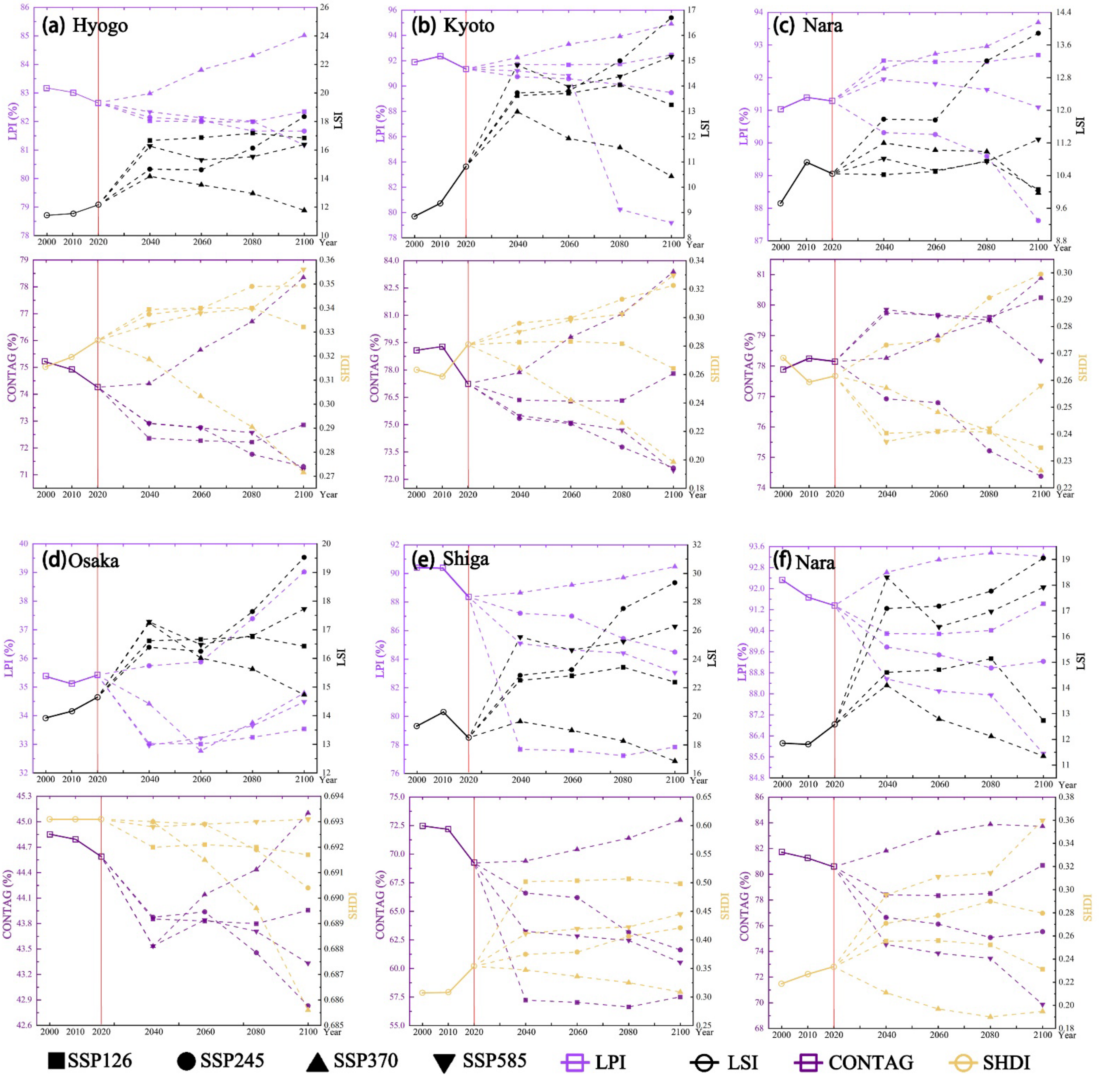

Figure 9. Changes in spatial pattern index of artificial surface from 2000 to 2100.

4.4. Important Cultivated Land Patches and Corridors Identification

The spatial patterns of cultivated land in each prefecture are characterized by core areas, edges, perforations, and a small portion of linear patterns (such as loops, bridges, and branches) that account for less than 30% (Figure S3). By 2100, in the SSP126 scenario, Shiga, Kyoto, and Hyogo experience significant reductions in cultivated land area (Figure 10). Specifically, in Shiga and the northern region of Kyoto, the core area decreases significantly, the number of islets increases, and there is severe fragmentation of cultivated land patches. In the SSP245 and SSP370 scenarios, the area of cultivated land decreases, and the cultivated land distribution of MSPA classes was similar. In the SSP585 scenario, cultivated land increases in all prefectures except Shiga. The core, edge, and perforation areas account for more than 65% of the total area, while islets make up less than 6%. This indicates a higher level of integrity in cultivated land.

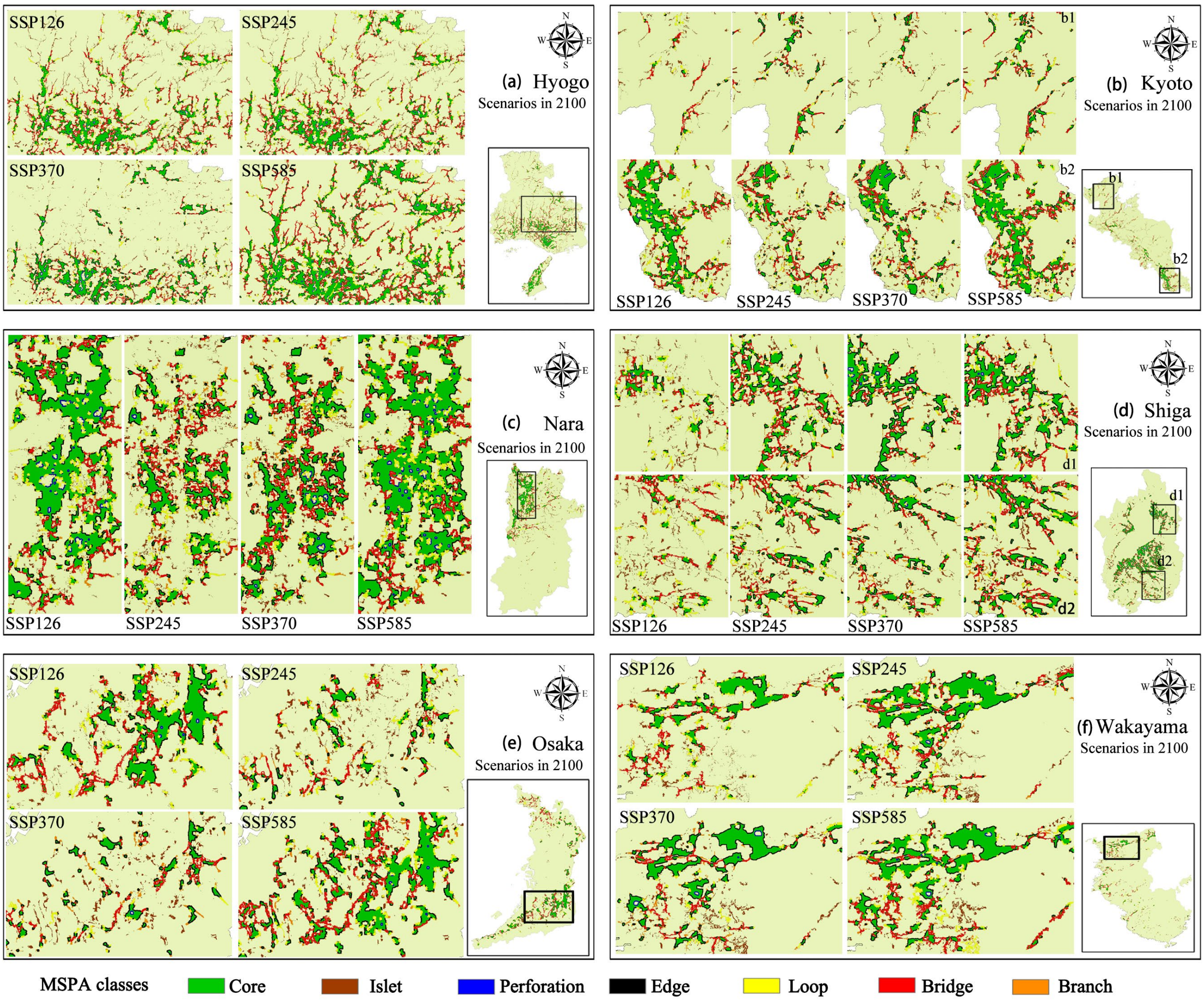

Figure 10. MSPA classes of cultivated land in four scenarios at 2100.

Within the Kinki metropolitan area, the majority of cultivated land exists in the form of important patches and corridors, accounting for over 90% of the total area of cultivated land in most prefectures; meanwhile, the number is less than 25%. The number of patches is generally smaller than that of corridors, while the area of patches is larger than corridors (Figure 11). Hyogo stands out with the largest area and the numbers of important patches and corridors, while Osaka has the lowest. When comparing the numbers and areas from 2000 to 2020, Hyogo, Osaka, and Wakayama exhibited relatively stable fluctuations, with an increase in area under the SSP126 scenario from 2020 to 2060. Conversely, the number gradually decreased in the remaining prefectures, year by year. Under the SSP245 scenario, both the numbers and areas of important patches and corridors in all of the prefectures showed relatively minor fluctuations from 2020 to 2060. By 2100, the areas decreased in all of the prefectures, while the numbers increased significantly in Shiga and Wakayama. In the SSP370 scenario, the Hyogo and Kyoto prefectures experienced the most rapid decline in area, while the other prefectures showed smaller changes from 2040 to 2080, until 2100, when they begin to decline more significantly. Under the SSP585 scenario, both the areas and the amounts increased in all of the prefectures except for Shiga.

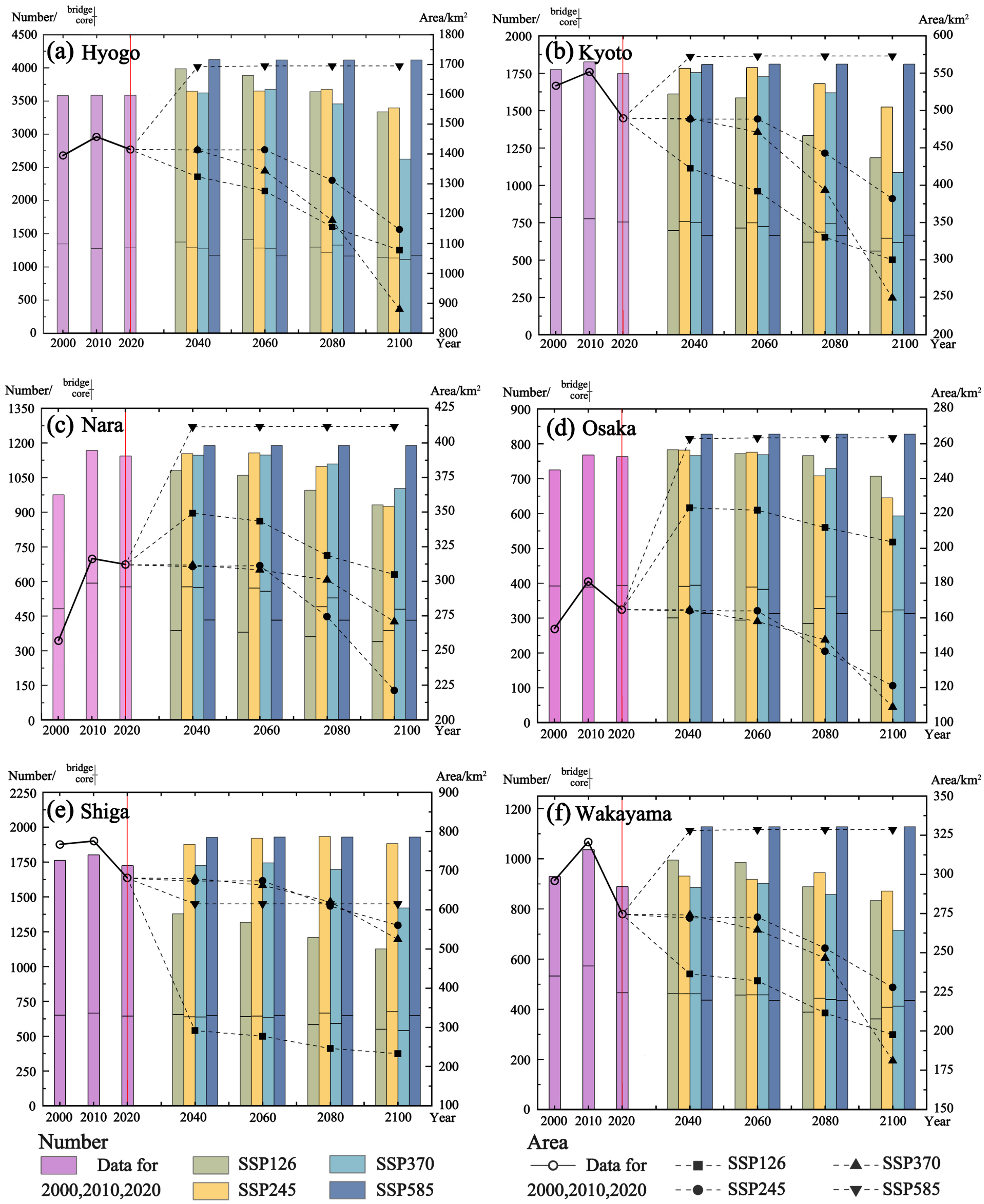

Figure 11. Changes in important cultivated land patches and corridors in six prefectures from 2000 to 2100.

4.5. Forest MSPA Classes Change and the Influence on CS Changes

The core is the largest area among all of the forest MSPA classes (Figure S4). The Kinki metropolitan area has good forest integrity. The forest area increased in all of the scenarios except for SSP585. Among the prefectures, the core and edge areas increased more, while the areas of MSPA linear classes fluctuated less. However, there were some exceptions, such as the MSPA class changes in Nara under SSP370. While the areas of its core, edge, and islet decreased, the increase in bridges led to an increase in forest area. Furthermore, while the forest area of SSP585 decreased, the forest core remained stable in most prefectures, such as Hyogo, Kyoto, and Shiga, where the woodland acreage decreased while the core area rose.

Among different land types, forests, grasslands, and croplands exhibit high carbon density, with forests having the highest. In this study, 24 CS changes and forest MSPA changes were extracted from six prefectures under the four scenarios to explore the relationship between forest morphological characteristics and CS changes. The correlation analysis revealed that not all MSPA classes had a significant impact on CS changes (Figure 12). For instance, only the branch area had a significant influence on CS changes under the SSP126 scenario. Additionally, not all MSPA classes necessarily contributed to the CS density increase. In all of the cases, the forest branch area was negatively associated with CS change; this result means that in most cases, the increase in branch area is related to changes in other MSPA classes in forests. The changes in CS can reflect the conversion patterns of forest morphology. For instance, in three scenarios, the CS change exhibited a positive correlation with core areas, indicating that the prefectures of metropolitan Kinki focused on maintaining and constructing core areas in forest development, thereby integrating or modifying the fragmented MSPA classes.

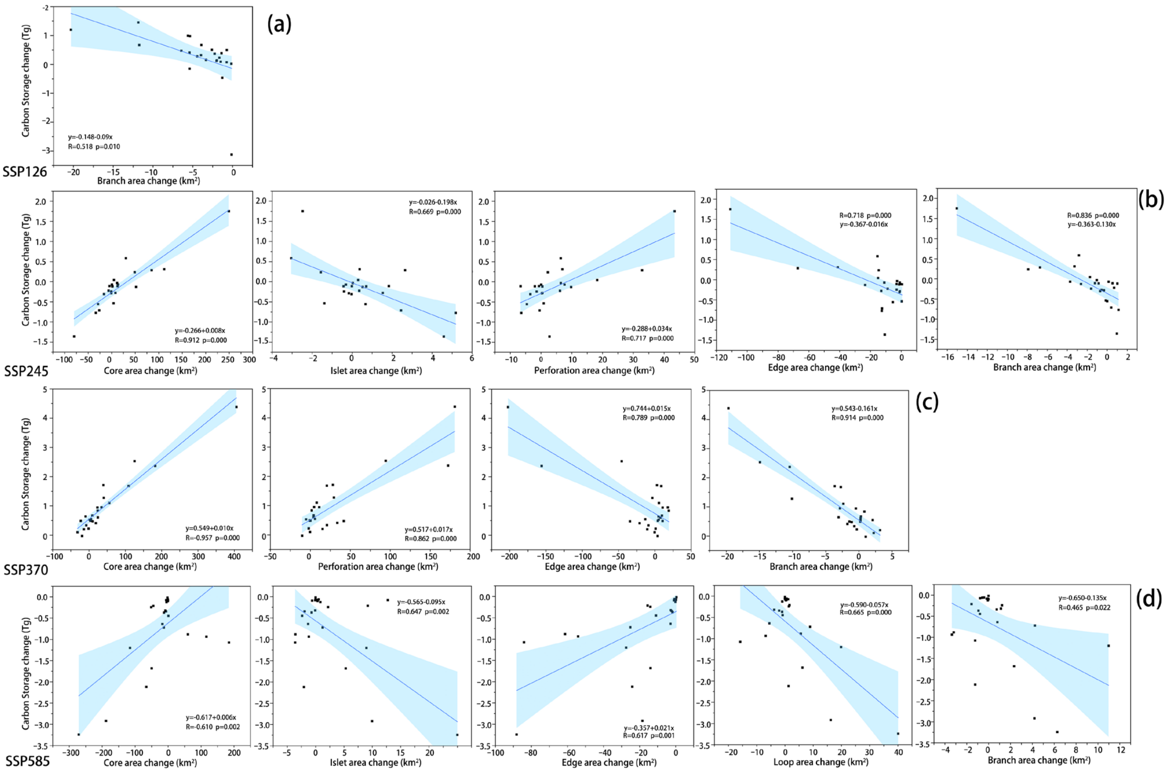

Figure 12. Correlations between CS with MSPA classes changes in forests in metropolitan Kinki. The shaded areas represent 95% confidence intervals ((**a**) SSP126, (**b**) SSP245, (**c**) SSP370, (**d**) SSP585).

5. Discussion

5.1. The Driving Factors Influencing LULC Change

This study simulated and analyzed the LULC changes in the Kinki metropolitan area under various climates and socioeconomic situations (Figure 13). Under the scenarios of population decrease, economic change, and global warming, cultivated land, forests, and artificial surfaces are the main types of LULC changes in 2040, 2060, 2080, and 2100 (Table 4). In addition, the overlap probability of 25 driving factors with growth areas over 2020–2100 shows that the growth areas of the three LULC types are all strongly related to climate factors and socioeconomic factors. Economic development paths and global climate change will affect future LULC [12,19,39]. In addition to climatic and socioeconomic factors, soil factors such as sand content and soil content also have a great effect on cultivated land growth under the SSP126, SSP245, and SSP370 scenarios. This result shows that favorable soil conditions are necessary for cultivated land development in regions where cultivated land continues to decline [58,59]. In the SSP585 scenario, the spatial accessibility factors overlap significantly with the cultivated land growth. This result shows that cultivated land growth is in fact directly tied to human cropland needs and activities [4,12]. The driving factors influencing forest growth in the four scenarios are highly consistent, with GDP, climate, and soil factors dominating and human activity-related factors playing a minor role. It reflects that superior geographic conditions and an economic base play a role in the restoration and creation of forests in the Kinki metropolitan area. Furthermore, as urban construction and road planning improve while the forest ecosystem is in a superior state, the impact of human activity on forest ecosystems becomes less significant. The distribution of artificial surface growth areas is highly consistent with the GDP and population. Metropolitan areas with high population densities and high economic development levels require more land for production, living, and working [60]. Furthermore, there is consistency between artificial surface growth and climatic factors such as precipitation. The urban expansion will lead to more GHG emissions and CS reduction, which means climate change and human activities are closely intertwined [61]. This study also discovered that the growth in artificial surface areas is related to roadways, open water, and topography. Previous studies explored the main factors driving urban expansion by determining the distances between metropolitan areas and roads, open water, and so on [62,63]. It indicates that good infrastructure services are the foundation of urban construction.

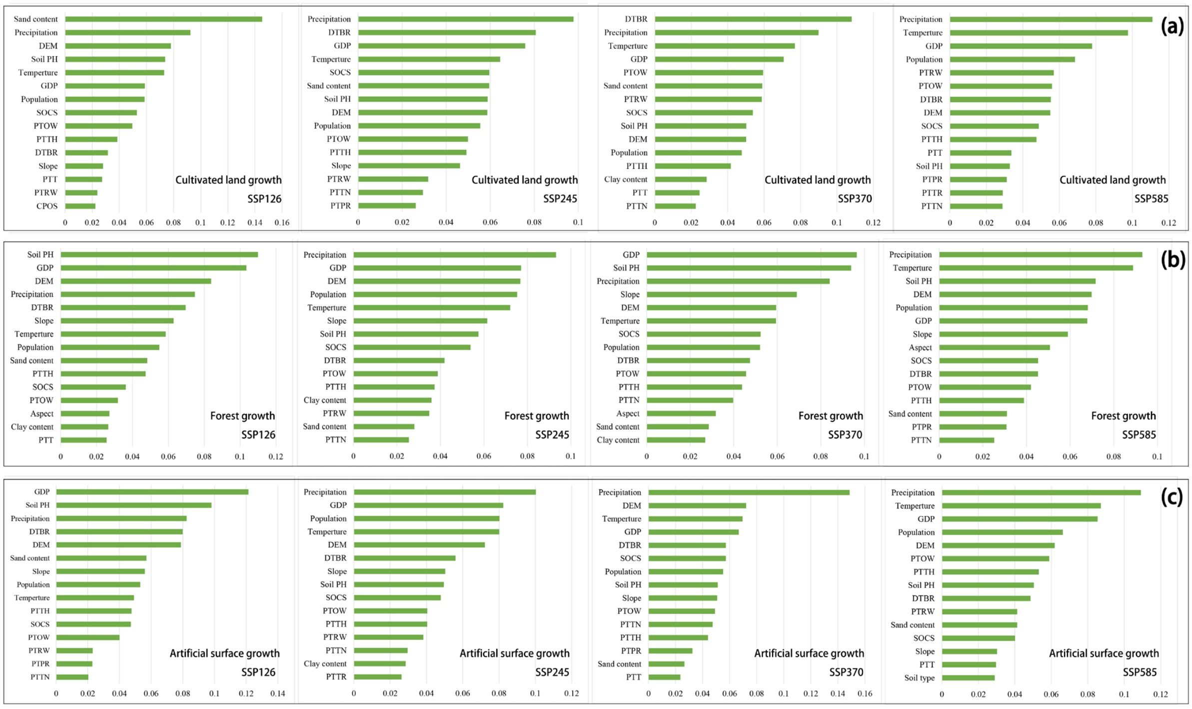

Figure 13. The contribution of each variable to the growth of three LULC types (the top 15 factors were chosen). (**a**) Cultivated land growth, (**b**) forest growth, (**c**) artificial surface growth. DTBR: depth to bedrock, CPOS: cumulative probability of organic soil, SOCS: soil organic carbon stock. PTTH: proximity to town hall, PTTN: proximity to transportation node, PTRW: proximity to railway, PTT: proximity trunk/motorway, PTPR: proximity to primary road, PTTR: proximity to tertiary road, PTOW: proximity to open water.

5.2. The Application of Future LULC in Wide-Area Planning

The future LULC results for most scenarios in the Kinki metropolitan area are in line with the current development trends, such as the gradual decrease in cultivated land and the increase in forested areas (Table 4) [59,64]. These findings are consistent with the results of previous LULC simulations conducted in Japan [27,65]. Additionally, the higher carbon densities observed in forests, attributed to differences in plant growth and underground soil characteristics [42,66], indicate a strong potential for the carbon density to increase in the future of the Kinki metropolitan area. In this context, the emphasis of future climate regulation within the Kinki metropolis will be on enhancing climate regulation within densely developed urban areas. The expansion of the artificial surfaces, coupled with the establishment of urban forests, holds the potential to ameliorate the thermal climate within the city. Furthermore, a noticeable surge in the volume of studies concentrating on LULC simulations has been evident in recent years. As researchers delve into this field, it becomes crucial to not only analyze the outcomes of these studies, but also to discuss their practical implications.

For forested land, since 1968, urban development in Japan has been strictly regulated [26,66], and the LULC has been carefully planned and governed by legislation [67]. In terms of forests, until 2100, the future LULC changes under the four scenarios have less disruptive impacts on the conservation areas established in the Regional Green Space Planning; forested areas within artificial surface areas are not significantly encroached upon (Figure 14). We also found that with the exception of the SSP585 scenario, the rise in forests is paralleled by a decline in cultivated land in most scenarios. This trend could be attributed to the ongoing decrease in Japan's population, leading to farmland abandonment. Concurrently, the demand for land for construction has reached a saturation point. Consequently, the abandoned farmland is translated into forest. Based on this background, it is important to note that while the Regional Green Space Planning of each prefecture has well-defined boundaries for conservation areas, there is a lack of clarity when it comes to delineating future conservation areas and optimizing existing conservation area boundaries. To address this challenge, the characteristics of forest development in prefectures under the four scenarios serve as valuable references for optimizing and delineating conservation areas. In addition, within the Kinki metropolitan area, there are interconversions between different MSPA classes of forests, and linear forests are identified as a relatively unstable category. By analyzing the dynamic changes of linear forests, we can ensure the connectivity between large forest patches by defining the boundaries of forest corridor protection.

For artificial surfaces, under all four of the scenarios, urban expansion tends to be concentrated in the central region of the Kinki metropolitan area, the north of Wakayama, and the southeast of Lake Biwa in Shiga (Figures 5 and 15); these results are consistent with the development areas identified in the Kinki Area Adjustment plan (Figure 9). In the future, the expansion of artificial surface area in the Kinki metropolitan is projected to continue under all of the scenarios except for SSP370. While Japan's population is experiencing a decline, and the immediate demand for artificial surfaces is not pressing, it is plausible that adjustments in the development of artificial surfaces are taking place in accordance with policy shifts. Such changes in land use functions could be contributing to the abandonment of certain artificial surfaces. Additionally, the significant economic costs associated with demolishing existing structures or concrete surfaces have likely contributed to these areas persisting as artificial surfaces.

In addition, there are notable variations in the development characteristics among different prefectures within the region. This study identifies three categories of cities based on the fluctuating indices related to the spatial distribution change of artificial surfaces, including (1) Hyogo, Shiga, and Wakayama; (2) Kyoto and Nara; and (3) Osaka. These differences reflect the functional characteristics and regional positioning of different prefectures. It emphasizes the importance of synergistic planning among cities to ensure coordinated and sustainable regional development.

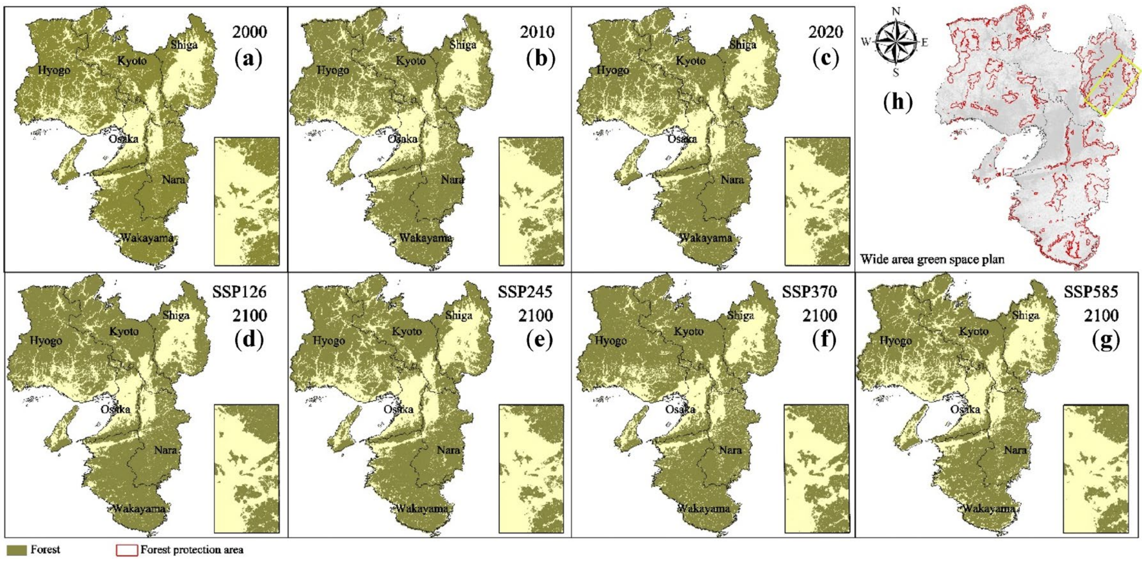

Figure 14. Distributions of forest in 2000–2020 and 2100 under four SSP–RCP scenarios ((**a**) 2000, (**b**) 2010, (**c**) 2020, (**d**) SSP126 in 2100, (**e**) SSP245 in 2100, (**f**) SSP370 in 2100, (**g**) SSP585 in 2100, (**h**) wide-area green space plan).

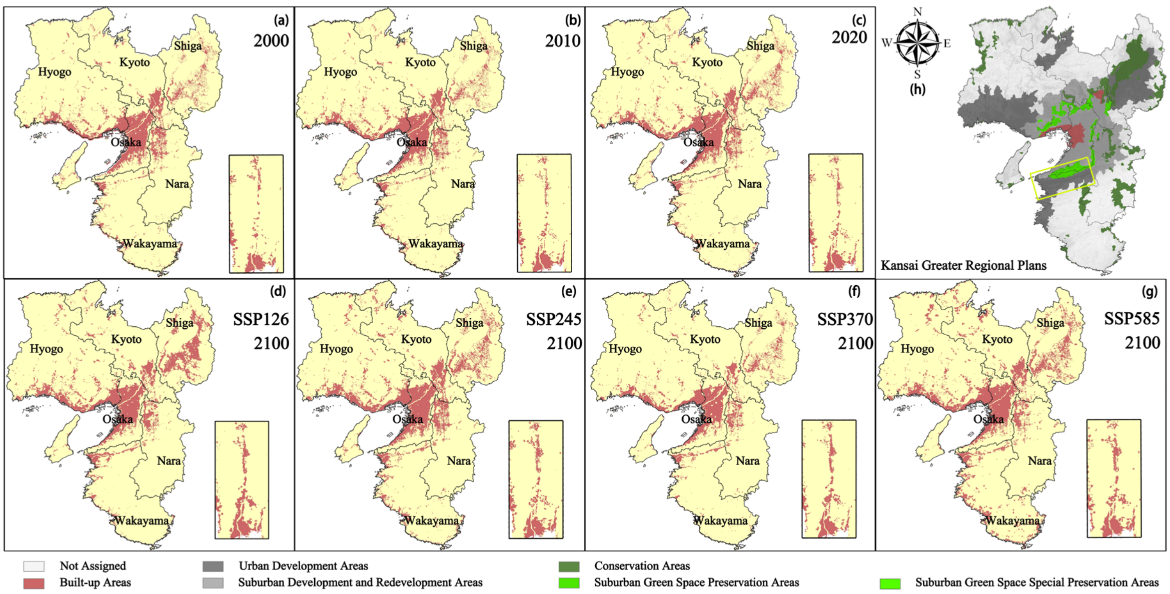

Figure 15. Distribution of artificial surface areas in 2000–2020 and 2100 under four SSP–RCP scenarios ((**a**) 2000, (**b**) 2010, (**c**) 2020, (**d**) SSP126 in 2100, (**e**) SSP245 in 2100, (**f**) SSP370 in 2100, (**g**) SSP585 in 2100, (**h**) Kansai greater reginal plans).

For cultivated land, Japan is a heavily depopulated country in rural areas suffering from serious abandonment and reduced cultivated land [68]. In addition, food shortages are expected to become more serious due to extreme weather caused by global warming. Along with progress in the development of new crops and approaches to address food problems, it is also important to discuss conservation policies for cultivated land within the Agricultural Promotion Regional System and the Agricultural Land Conversion Permission System [69]. In recent years, there has been an increase in studies on how to use abandoned cultivated land, improve agriculture production, and protect cultivated land [70,71]. Shiga, Hyogo, and Kyoto are at risk of seriously decreasing cultivated land by 2100 under several scenarios. This study identified important cultivated land in two different forms, patches and corridors, and clarified the locations of important patches and their changes between

2000 and 2100. We provide basic data for dynamic monitoring of cultivated land patches based on our research results.

6. Conclusions

The CMIP6 has been widely adopted and used in LULC simulations in response to complex climate, social, and economic changes. This study focuses on the Kinki metropolis of Japan, which is characterized by significant aging and slow urbanization. This study simulated and analyzed LULC and CS changes for the years 2040, 2060, 2080, and 2100 using the PLUS–InVEST model. The results reveal that, except under the SSP585 scenario, the cultivated land area in the Kinki metropolis will decrease, while the forest area will increase. The artificial surface area decreases only in the SSP370 scenario. There are consistent change characteristics between the CS change and forest area change. Based on wide-area planning and the LULC management policies in metropolitan Kinki, this study further analyzed and discussed the spatial patterns of artificial surfaces, the identification of important patches and corridors of cultivated land, and the dynamic changes in quantity and area, as well as the transformation patterns of forest MSPA classes. The above analysis provides a reference for LULC management and planning policy formulation in the Kinki metropolitan area in the face of different future climate changes and socioeconomic scenarios.

The LULC simulation results of this study serve as fundamental information for collaborative urban planning, the planning and adjustment of nature reserve areas, and the dynamic regulation and protection of cultivated land. This study contributes to a comprehensive understanding of the future dynamic changes in the LULC area in metropolitan Kinki under different climate change and economic development scenarios, emphasizing the significance of formulating localized land management strategies and providing valuable references for policymakers and land managers.

Supplementary Materials: The following supporting information can be downloaded at: https://www.mdpi.com/article/10.3390/land12091722/s1, Figure S1: The planning system for national land use in Japan; Figure S2: MSPA classes of cultivated land in four scenarios in 2100; Figure S3: MSPA classes change of forest in prefectures under four scenarios. Figure S4. MSPA classes change of forest in prefectures under four scenarios. Table S1. Some scenarios used in this study ("√"represents we have chosen). Table S2. Comparison between actual LULC in 2020 and simulation result in 2020.

Author Contributions: Y.X.: Conceptualization, methodology; formal analysis; visualization; writing—original draft and revise the draft. K.F.: Writing—review. W.W.: Writing—review. S.S.: Funding acquisition; resources; writing—review. All authors have read and agreed to the published version of the manuscript.

Funding: This research was funded by the Grant-in-Aid for Scientific Research (B) [No. 21H02224] and Xie is financially and administratively supported by both the Ministry of Education, Culture, Sports, Science and Technology of Japan (MEXT) and the China Scholarship Council (CSC) [No.202006240035] for his doctoral research.

Data Availability Statement: The data presented in this study are available on request from the corresponding author. The data are not publicly available due to privacy.

Conflicts of Interest: The authors declare no conflict of interest.

References

1. IPCC. *Climate Change*; IPCC: Geneva, Switzerland, 2023. Available online: https://www.ipcc.ch/report/ar6/syr/downloads/report/IPCC_AR6_SYR_SPM.pdf (accessed on 2 May 2023).
2. Li, C.; Wu, Y.; Gao, B.; Zheng, K.; Wu, Y.; Li, C. Multi-Scenario Simulation of Ecosystem Service Value for Optimization of Land Use in the Sichuan-Yunnan Ecological Barrier, China. *Ecol. Indic.* **2021**, *132*, 108328. [CrossRef]
3. Wang, Z.; Li, X.; Mao, Y.; Li, L.; Wang, X.; Lin, Q. Dynamic Simulation of Land Use Change and Assessment of Carbon Storage Based on Climate Change Scenarios at the City Level: A Case Study of Bortala, China. *Ecol. Indic.* **2022**, *134*, 108499. [CrossRef]
4. Tian, L.; Tao, Y.; Fu, W.; Li, T.; Ren, F.; Li, M. Dynamic Simulation of Land Use/Cover Change and Assessment of Forest Ecosystem Carbon Storage under Climate Change Scenarios in Guangdong Province, China. *Remote Sens.* **2022**, *14*, 2330. [CrossRef]

5. Xiang, S.; Wang, Y.; Deng, H.; Yang, C.; Wang, Z.; Gao, M. Response and Multi-Scenario Prediction of Carbon Storage to Land Use/Cover Change in the Main Urban Area of Chongqing, China. *Ecol. Indic.* **2022**, *142*, 109205. [CrossRef]
6. Raum, S.; Hand, K.L.; Hall, C.; Edwards, D.M.; O'Brien, L.; Doick, K.J. Achieving Impact from Ecosystem Assessment and Valuation of Urban Greenspace: The Case of i-Tree Eco in Great Britain. *Landsc. Urban Plan.* **2019**, *190*, 103590. [CrossRef]
7. Ul Din, S.; Mak, H.W.L. Retrieval of Land-Use/Land Cover Change (LUCC) Maps and Urban Expansion Dynamics of Hyderabad, Pakistan via Landsat Datasets and Support Vector Machine Framework. *Remote Sens.* **2021**, *13*, 3337. [CrossRef]
8. Xiong, N.; Yu, R.; Yan, F.; Wang, J.; Feng, Z. Land Use and Land Cover Changes and Prediction Based on Multi-Scenario Simulation: A Case Study of Qishan County, China. *Remote Sens.* **2022**, *14*, 4041. [CrossRef]
9. Bagan, H.; Yamagata, Y. Land-Cover Change Analysis in 50 Global Cities by Using a Combination of Landsat Data and Analysis of Grid Cells. *Environ. Res. Lett.* **2014**, *9*, 064015. [CrossRef]
10. Güneralp, B.; Reba, M.; Hales, B.U.; Wentz, E.A.; Seto, K.C. Trends in Urban Land Expansion, Density, and Land Transitions from 1970 to 2010: A Global Synthesis. *Environ. Res. Lett.* **2020**, *15*, 044015. [CrossRef]
11. Shi, X.; Matsui, T.; Haga, C.; Machimura, T.; Hashimoto, S.; Saito, O. A Scenario- and Spatial-Downscaling-Based Land-Use Modeling Framework to Improve the Projections of Plausible Futures: A Case Study of the Guangdong–Hong Kong–Macao Greater Bay Area, China. *Sustain. Sci.* **2021**, *16*, 1977–1998. [CrossRef]
12. Popp, A.; Calvin, K.; Fujimori, S.; Havlik, P.; Humpenöder, F.; Stehfest, E.; Bodirsky, B.L.; Dietrich, J.P.; Doelmann, J.C.; Gusti, M.; et al. Land-Use Futures in the Shared Socio-Economic Pathways. *Glob. Environ. Chang.* **2017**, *42*, 331–345. [CrossRef]
13. Eyring, V.; Bony, S.; Meehl, G.A.; Senior, C.A.; Stevens, B.; Stouffer, R.J.; Taylor, K.E. Overview of the Coupled Model Intercomparison Project Phase 6 (CMIP6) Experimental Design and Organization. *Geosci. Model Dev.* **2016**, *9*, 1937–1958. [CrossRef]
14. Tebaldi, C.; Debeire, K.; Eyring, V.; Fischer, E.; Fyfe, J.; Friedlingstein, P.; Knutti, R.; Lowe, J.; O'Neill, B.; Sanderson, B.; et al. Climate Model Projections from the Scenario Model Intercomparison Project (ScenarioMIP) of CMIP6. *Earth Syst. Dyn.* **2021**, *12*, 253–293. [CrossRef]
15. O'Neill, B.C.; Tebaldi, C.; Van Vuuren, D.P.; Eyring, V.; Friedlingstein, P.; Hurtt, G.; Knutti, R.; Kriegler, E.; Lamarque, J.-F.; Lowe, J.; et al. The Scenario Model Intercomparison Project (ScenarioMIP) for CMIP6. *Geosci. Model Dev.* **2016**, *9*, 3461–3482. [CrossRef]
16. Gong, L.; Zhang, X.; Pan, G.; Zhao, J.; Zhao, Y. Hydrological Responses to Co-Impacts of Climate Change and Land Use/Cover Change Based on CMIP6 in the Ganjiang River, Poyang Lake Basin. *Anthropocene* **2023**, *41*, 100368. [CrossRef]
17. Hurtt, G.C.; Chini, L.; Sahajpal, R.; Frolking, S.; Bodirsky, B.L.; Calvin, K.; Doelman, J.C.; Fisk, J.; Fujimori, S.; Klein Goldewijk, K.; et al. Harmonization of Global Land Use Change and Management for the Period 850–2100 (LUH2) for CMIP6. *Geosci. Model Dev.* **2020**, *13*, 5425–5464. [CrossRef]
18. Kumar, N.; Singh, V.G.; Singh, S.K.; Behera, D.K.; Gašparović, M. Modeling of Land Use Change under the Recent Climate Projections of CMIP6: A Case Study of Indian River Basin. *Environ. Sci. Pollut. Res.* **2023**. [CrossRef] [PubMed]
19. Liao, W.; Liu, X.; Xu, X.; Chen, G.; Liang, X.; Zhang, H.; Li, X. Projections of Land Use Changes under the Plant Functional Type Classification in Different SSP-RCP Scenarios in China. *Sci. Bull.* **2020**, *65*, 1935–1947. [CrossRef] [PubMed]
20. Nasiakou, S.; Vrahnakis, M.; Chouvardas, D.; Mamanis, G.; Kleftoyanni, V. Land Use Changes for Investments in Silvoarable Agriculture Projected by the CLUE-S Spatio-Temporal Model. *Land* **2022**, *11*, 598. [CrossRef]
21. Sobhani, P.; Esmaeilzadeh, H.; Mostafavi, H. Simulation and Impact Assessment of Future Land Use and Land Cover Changes in Two Protected Areas in Tehran, Iran. *Sustain. Cities Soc.* **2021**, *75*, 103296. [CrossRef]
22. Sun, J.; Zhang, Y.; Qin, W.; Chai, G. Estimation and Simulation of Forest Carbon Stock in Northeast China Forestry Based on Future Climate Change and LUCC. *Remote Sens.* **2022**, *14*, 3653. [CrossRef]
23. Liang, X.; Guan, Q.; Clarke, K.C.; Liu, S.; Wang, B.; Yao, Y. Understanding the Drivers of Sustainable Land Expansion Using a Patch-Generating Land Use Simulation (PLUS) Model: A Case Study in Wuhan, China. *Comput. Environ. Urban Syst.* **2021**, *85*, 101569. [CrossRef]
24. Gomes, E.; Inácio, M.; Bogdzevič, K.; Kalinauskas, M.; Karnauskaitė, D.; Pereira, P. Future Land-Use Changes and Its Impacts on Terrestrial Ecosystem Services: A Review. *Sci. Total Environ.* **2021**, *781*, 146716. [CrossRef] [PubMed]
25. Hou, Y.; Chen, Y.; Li, Z.; Li, Y.; Sun, F.; Zhang, S.; Wang, C.; Feng, M. Land Use Dynamic Changes in an Arid Inland River Basin Based on Multi-Scenario Simulation. *Remote Sens.* **2022**, *14*, 2797. [CrossRef]
26. Millward, H. Urban Containment Strategies: A Case-Study Appraisal of Plans and Policies in Japanese, British, and Canadian Cities. *Land Use Policy* **2006**, *23*, 473–485. [CrossRef]
27. Chen, Z.; Huang, M.; Zhu, D.; Altan, O. Integrating Remote Sensing and a Markov-FLUS Model to Simulate Future Land Use Changes in Hokkaido, Japan. *Remote Sens.* **2021**, *13*, 2621. [CrossRef]
28. Ito, J.; Nishikori, M.; Toyoshi, M.; Feuer, H.N. The Contribution of Land Exchange Institutions and Markets in Countering Farmland Abandonment in Japan. *Land Use Policy* **2016**, *57*, 582–593. [CrossRef]
29. Tsuchiya, S. *Facts and Considerations on the "Urbanization Rate" in Japan from the Perspective of Regional Economy*; Bank of Japan Working Paper Series; Bank of Japan: Tokyo, Japan, 2009; J-4; p. 37.
30. Chang, Q.; Liu, X.; Wu, J.; He, P. MSPA-Based Urban Green Infrastructure Planning and Management Approach for Urban Sustainability: Case Study of Longgang in China. *J. Urban Plann. Dev.* **2015**, *141*, A5014006. [CrossRef]
31. Kang, S.; Kim, J.-O. Morphological Analysis of Green Infrastructure in the Seoul Metropolitan Area, South Korea. *Landsc. Ecol. Eng.* **2015**, *11*, 259–268. [CrossRef]

32. Wang, K.; Li, Z.; Zhang, J.; Wu, X.; Jia, M.; Wu, L. Built-up Land Expansion and Its Impacts on Optimizing Green Infrastructure Networks in a Resource-Dependent City. *Sustain. Cities Soc.* **2020**, *55*, 102026. [CrossRef]
33. Soille, P.; Vogt, P. Morphological Segmentation of Binary Patterns. *Pattern Recognit. Lett.* **2009**, *30*, 456–459. [CrossRef]
34. Chen, M.; Dai, F.; Yang, B.; Zhu, S. Effects of Urban Green Space Morphological Pattern on Variation of PM2.5 Concentration in the Neighborhoods of Five Chinese Megacities. *Build. Environ.* **2019**, *158*, 1–15. [CrossRef]
35. Statistics Bureau of Japan 2020 Population Census. Available online: https://www.stat.go.jp/data/kokusei/2020/kekka/pdf/outline.pdf (accessed on 16 November 2022).
36. Wang, T.; Sun, F. Global Gridded GDP Data Set Consistent with the Shared Socioeconomic Pathways. *Sci. Data* **2022**, *9*, 221. [CrossRef] [PubMed]
37. Kummu, M.; Taka, M.; Guillaume, J.H.A. Gridded Global Datasets for Gross Domestic Product and Human Development Index over 1990–2015. *Sci. Data* **2018**, *5*, 180004. [CrossRef] [PubMed]
38. Li, J.; Chen, X.; Kurban, A.; Van de Voorde, T.; De Maeyer, P.; Zhang, C. Coupled SSPs-RCPs Scenarios to Project the Future Dynamic Variations of Water-Soil-Carbon-Biodiversity Services in Central Asia. *Ecol. Indic.* **2021**, *129*, 107936. [CrossRef]
39. Riahi, K.; van Vuuren, D.P.; Kriegler, E.; Edmonds, J.; O'Neill, B.C.; Fujimori, S.; Bauer, N.; Calvin, K.; Dellink, R.; Fricko, O.; et al. The Shared Socioeconomic Pathways and Their Energy, Land Use, and Greenhouse Gas Emissions Implications: An Overview. *Glob. Environ. Change* **2017**, *42*, 153–168. [CrossRef]
40. Lin, Z.; Peng, S. Comparison of Multimodel Simulations of Land Use and Land Cover Change Considering Integrated Constraints—A Case Study of the Fuxian Lake Basin. *Ecol. Indic.* **2022**, *142*, 109254. [CrossRef]
41. Sahle, M.; Saito, O.; Fürst, C.; Demissew, S.; Yeshitela, K. Future Land Use Management Effects on Ecosystem Services under Different Scenarios in the Wabe River Catchment of Gurage Mountain Chain Landscape, Ethiopia. *Sustain. Sci.* **2019**, *14*, 175–190. [CrossRef]
42. Li, K.; Cao, J.; Adamowski, J.F.; Biswas, A.; Zhou, J.; Liu, Y.; Zhang, Y.; Liu, C.; Dong, X.; Qin, Y. Assessing the Effects of Ecological Engineering on Spatiotemporal Dynamics of Carbon Storage from 2000 to 2016 in the Loess Plateau Area Using the InVEST Model: A Case Study in Huining County, China. *Environ. Dev.* **2021**, *39*, 100641. [CrossRef]
43. IPCC. 2006 IPCC Guidelines for National Greenhouse Gas Inventories. 2006. Available online: https://www.ipcc-nggip.iges.or.jp/public/2006gl/vol4.html (accessed on 5 April 2023).
44. Koga, N.; Smith, P.; Yeluripati, J.B.; Shirato, Y.; Kimura, S.D.; Nemoto, M. Estimating Net Primary Production and Annual Plant Carbon Inputs, and Modelling Future Changes in Soil Carbon Stocks in Arable Farmlands of Northern Japan. *Agric. Ecosyst. Environ.* **2011**, *144*, 51–60. [CrossRef]
45. Matsui, K.; Takata, Y.; Maejima, Y.; Kubotera, H.; Obara, H.; Shirato, Y. Soil Carbon and Nitrogen Stock of the Japanese Agricultural Land Estimated by the National Soil Monitoring Database (2015–2018). *Soil Sci. Plant Nutr.* **2021**, *67*, 633–642. [CrossRef]
46. Morisada, K.; Ono, K.; Kanomata, H. Organic Carbon Stock in Forest Soils in Japan. *Geoderma* **2004**, *119*, 21–32. [CrossRef]
47. Noguchi, K.; Hirai, K.; Takahashi, M.; Aizawa, S.; Itoh, Y. Effects of thinning on abovegroundcarbon and nitrogen dynamics ata sugi (Cryptomeriajaponica) plantation innorthern Kanto region, eastern Japan. *Bull. FFPRI* **2009**, *8*, 205–214.
48. Takahashi, M.; Ishizuka, S.; Ugawa, S.; Sakai, Y.; Sakai, H.; Ono, K.; Hashimoto, S.; Matsuura, Y.; Morisada, K. Carbon Stock in Litter, Deadwood and Soil in Japan's Forest Sector and Its Comparison with Carbon Stock in Agricultural Soils. *Soil Sci. Plant Nutr.* **2010**, *56*, 19–30. [CrossRef]
49. Matsuura, S.; Sasaki, H.; Kohyama, K. Organic Carbon Stocks in Grassland Soils and Their Spatial Distribution in Japan: Carbon Stocks in Japan's Grassland Soils. *Grassl. Sci.* **2012**, *58*, 79–93. [CrossRef]
50. Takahashi, T.; Amano, Y.; Kuchimura, K.; Kobayashi, T. Carbon Content of Soil in Urban Parks in Tokyo, Japan. *Landsc. Ecol. Eng.* **2008**, *4*, 139–142. [CrossRef]
51. McGarigal, K.; Marks, B.J. *FRAGSTATS: Spatial Pattern Analysis Program for Quantifying Landscape Structure*; U.S. Department of Agriculture, Forest Service, Pacific Northwest Research Station: Portland, OR, USA, 1995; p. PNW-GTR-351.
52. Jiao, M.; Hu, M.; Xia, B. Spatiotemporal Dynamic Simulation of Land-Use and Landscape-Pattern in the Pearl River Delta, China. *Sustain. Cities Soc.* **2019**, *49*, 101581. [CrossRef]
53. Yin, J.; Wu, X.; Shen, M.; Zhang, X.; Zhu, C.; Xiang, H.; Shi, C.; Guo, Z.; Li, C. Impact of Urban Greenspace Spatial Pattern on Land Surface Temperature: A Case Study in Beijing Metropolitan Area, China. *Landsc. Ecol.* **2019**, *34*, 2949–2961. [CrossRef]
54. Vogt, P.; Riitters, K.H.; Estreguil, C.; Kozak, J.; Wade, T.G.; Wickham, J.D. Mapping Spatial Patterns with Morphological Image Processing. *Landsc. Ecol.* **2007**, *22*, 171–177. [CrossRef]
55. Riitters, K.; Vogt, P.; Soille, P.; Estreguil, C. Landscape Patterns from Mathematical Morphology on Maps with Contagion. *Landsc. Ecol.* **2009**, *24*, 699–709. [CrossRef]
56. Xie, Y.; Wang, Q.; Xie, M.; Shibata, S. Construction Feasibility Evaluation for Potential Ecological Corridors under Different Widths: A Case Study of Chengdu in China. *Landsc. Ecol. Eng.* **2023**, *19*, 381–399. [CrossRef]
57. Dytham, C.; Forman, R.T.T. Land Mosaics: The Ecology of Landscapes and Regions. *J. Ecol.* **1996**, *84*, 787. [CrossRef]
58. Oda, K.; Rupprecht, C.; Tsuchiya, K.; McGreevy, S. Urban Agriculture as a Sustainability Transition Strategy for Shrinking Cities? Land Use Change Trajectory as an Obstacle in Kyoto City, Japan. *Sustainability* **2018**, *10*, 1048. [CrossRef]
59. Takata, Y.; Obara, H.; Nakai, M.; Kohyama, K. Process of the decline in the cultivated soil area with land use changes in Japan. *Jpn. Soc. Soil Sci. Plant Nutr.* **2011**, *82*, 15–24.

60. Chen, G.; Li, X.; Liu, X.; Chen, Y.; Liang, X.; Leng, J.; Xu, X.; Liao, W.; Qiu, Y.; Wu, Q.; et al. Global Projections of Future Urban Land Expansion under Shared Socioeconomic Pathways. *Nat. Commun.* **2020**, *11*, 537. [CrossRef]
61. Wang, R.; Murayama, Y. Geo-Simulation of Land Use/Cover Scenarios and Impacts on Land Surface Temperature in Sapporo, Japan. *Sustain. Cities Soc.* **2020**, *63*, 102432. [CrossRef]
62. Fang, S.; Gertner, G.Z.; Sun, Z.; Anderson, A.A. The Impact of Interactions in Spatial Simulation of the Dynamics of Urban Sprawl. *Landsc. Urban Plan.* **2005**, *73*, 294–306. [CrossRef]
63. Salem, M.; Tsurusaki, N.; Divigalpitiya, P. Analyzing the Driving Factors Causing Urban Expansion in the Peri-Urban Areas Using Logistic Regression: A Case Study of the Greater Cairo Region. *Infrastructures* **2019**, *4*, 4. [CrossRef]
64. Kobayashi, Y.; Higa, M.; Higashiyama, K.; Nakamura, F. Drivers of Land-Use Changes in Societies with Decreasing Populations: A Comparison of the Factors Affecting Farmland Abandonment in a Food Production Area in Japan. *PLoS ONE* **2020**, *15*, e0235846. [CrossRef]
65. Shoyama, K.; Matsui, T.; Hashimoto, S.; Kabaya, K.; Oono, A.; Saito, O. Development of Land-Use Scenarios Using Vegetation Inventories in Japan. *Sustain. Sci.* **2019**, *14*, 39–52. [CrossRef]
66. Takeshi, M.; Toshikazu, A.; Bunpei, N.; Toshiya, M.; Shu, H. Study on Problem of Improvement Method for Infrastructure to Expanded Urban Area being secured only by District Plan. *J. City Plan. Inst. Jpn.* **2007**, *42*, 733–738. [CrossRef]
67. Seta, F. An Empirical Study on the Geographical Specification on National and Regional Plans in Japan: A Case Study of Kinki Area Regional Plan in National Spatial Strategies. *Toshi Keikaku Rombunshu* **2010**, *45*, 47–53. [CrossRef]
68. Su, G.; Okahashi, H.; Chen, L. Spatial Pattern of Farmland Abandonment in Japan: Identification and Determinants. *Sustainability* **2018**, *10*, 3676. [CrossRef]
69. Van Dijk, M.; Morley, T.; Rau, M.L.; Saghai, Y. A Meta-Analysis of Projected Global Food Demand and Population at Risk of Hunger for the Period 2010–2050. *Nat. Food* **2021**, *2*, 494–501. [CrossRef]
70. Hanioka, M.; Yamaura, Y.; Senzaki, M.; Yamanaka, S.; Kawamura, K.; Nakamura, F. Assessing the Landscape-Dependent Restoration Potential of Abandoned Farmland Using a Hierarchical Model of Bird Communities. *Agric. Ecosyst. Environ.* **2018**, *265*, 217–225. [CrossRef]
71. Nishihara, M. Real Option Valuation of Abandoned Farmland. *Rev. Financ. Econ.* **2012**, *21*, 188–192. [CrossRef]